Chapter IV

Chapter IV

Synthesis & Characterisation of Osmium (III) Complexes

4.1. Review of Literature

Osmium is the densest and hardest of the VIII B group metals, it is often alloyed with other platinum group metals such as platinum and iridium. Osmium is an excellent conductor of electricity, effective oxidation catalyst and also used in the field of fuel cells and forensic science.

Ramadan M. Ramadan *et al.*,[1] have reported the reaction of trinuclear clusters $M_3(CO)_{12}$ (M = Os) with 2,3-dihydroxyquinoxaline to give substituted mononuclear product. The complex **130** was trigonalbipyramidal structure with two CO molecules directly bonded to the osmium ion and confirmed by IR spectroscopy.

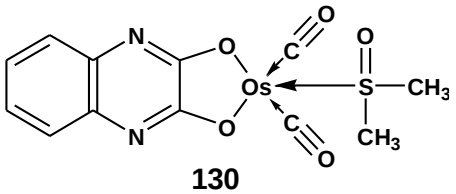

130

A series of osmium (VI) nitrido complexes containing Schiff base ligands was synthesised by the reaction of ligand with $[NBun_4][Os^{VI}(N)Cl_4]$ in the presence of 2,6-dimethylpyridine done by Tsz-Wing Wong *et al.*[2] The structure of the complexes was confirmed by spectral and X-ray crystallographic studies. The cyclic voltammteric studies confirmed that the complexes undergo reversible reaction.

Anindya Das *et al.*,[3] have synthesized and characterized three osmium complexes of type $[Os(PPh_3)_2(N\text{-}N)Br_2]$, where N-N=2,2'-bipyridine (bpy), 4,4'- dimethyl 2,2'–bipyridine (Me_2bpy) and 1,10-phenanthroline (phen) systems. The two bromide atoms present in the complexes easily underwent substitution reaction with other anionic ligands to produce the complexes of $[Os(PPh_3)_2(phen)(L)]^+$ type and the complexes were isolated as salt.

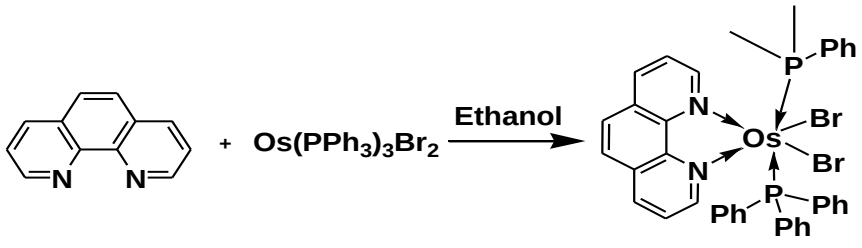

131 **132** **133**

Partha Majumdar *et al.*,[4] have prepared a series of trinuclear complexes of ruthenium and osmium bearing the terminal ligands 2-(phenylazo) pyridine triphenylphosphine and the bridging ligand 2,2-biimidazolate. The trinuclear complexes were confirmed by mass spectral studies and cyclic voltammetric studies.

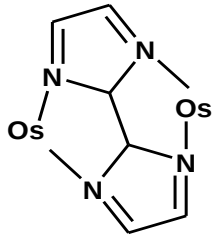

134

Bikash Kumar Panda *et al.*,[5] studied the reaction between osmium monocarbonyl system with CO at one atm. Pressure, which yielded yellow coloured dicarbonyl osmium complex.

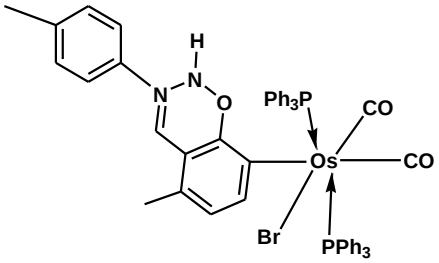

135

The study of variable coordination mode of chloroanilic acid with osmium (II) complexes $[Os(bpy)_2(Br_2)]$ was reported by Parna Gupta *et al*.[6] The chloroanilic acid acts both tetradenate as well as bidenate ligand. The structures of the complexes were confirmed by single X ray crystallographic studies.

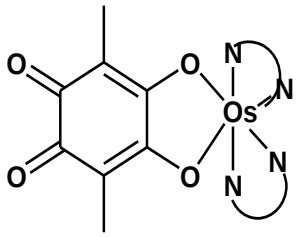

136

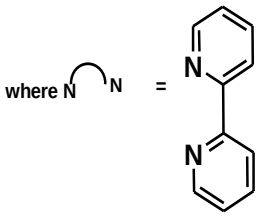

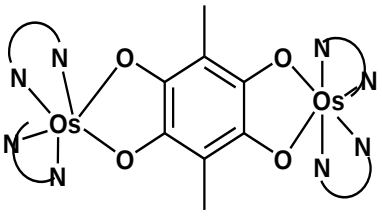

137

The dinuclear osmium(III) species $(C_5Me_5)_2Os_2Br_4$ **(140)** a mono(pentamethyl - cyclopentadienyl) complex was prepared by the reaction of H_2OsBr_6**(138)** with C_5Me_5H **(139)** in *tert*-butyl alcohol by Christopher L. Gross *et al*,[7] The single X-ray crystallographic studies revealed that the complex is half array sandwich and the distance between the terminal Os-Br bond is longer than bridging system.

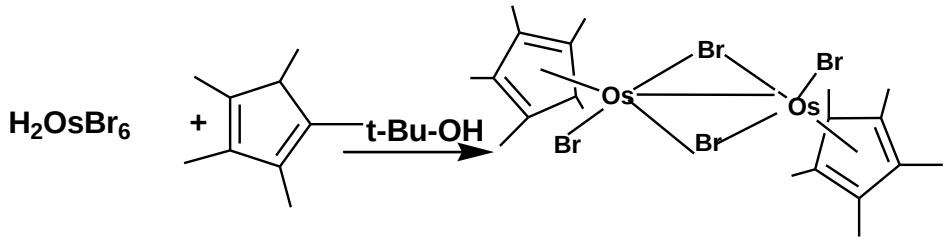

138 **139** **140**

Iryna Stepanenko *et al.*,[8] prepared the osmium (III) complexes containing azole ligand and compared their antiproliferativity with ruthenium (III) complex. Osmium (III) complex showed higher activity in all the three cancer cell line and less cytotoxic than Ru(III) complex.

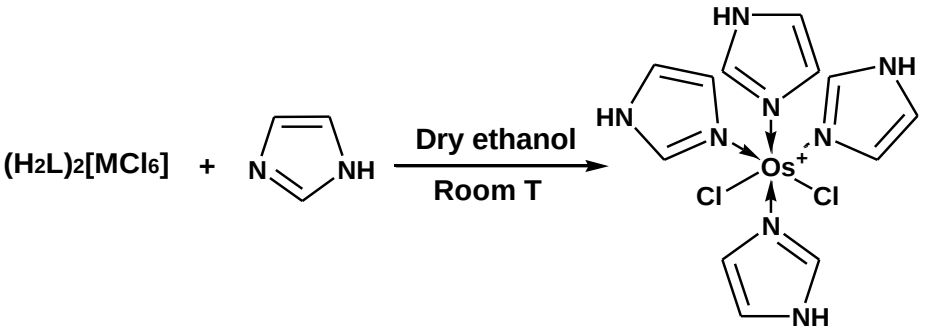

141 **142** **143**

Lukas *et al.,* [9] have synthesised and characterised a series of Ru(II) and Os(III) arene complexes containing the substitution at 8th position in the indolo quinoline system. The synthesised complexes are soluble in biological media and were analysed for antiproliferative activity of A549, CH1 and SW480 cancer cell lines and proved that the chloro group at 8th position is highly active 2nd position of quinoline systems.

Lukas K *et al.*,[10] have reported the synthesis and characterization of Os(III) complexes containing indolo[3,2-c]quinoline ligand **(144)** systems. The complexes were

subjected to antiproliferative activity against three human cancer cell lines and they exhibit IC_{50} values at low micromolar range.

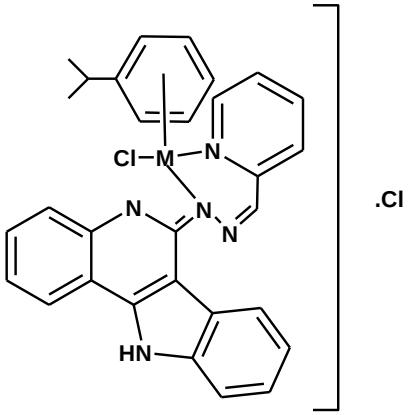

144

where M=Os

Soumik *et al.*,[11] have reported the reaction of a series of tripodal ligands, with $[M(PPh_3)_2Cl_2]$ (where M = Ru, Os). The reaction yielded a complexes of the type $[M^{III}L]$ or $[M^{II}L](BPh_4)_2$. All the synthesized compounds have been characterized by various spectroscopic methods and DFT calculations were performed to attain optimized geometry of all the metal complexes.

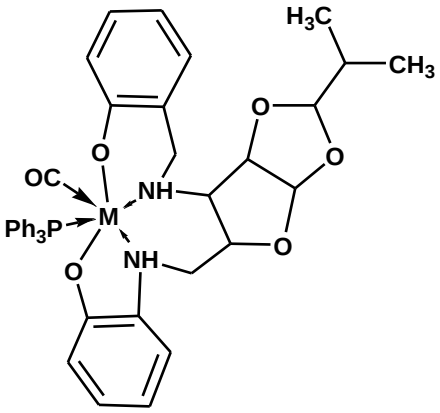

145

where M= Ru, Os

Osmium and ruthenium nitrosyl complexes bearing azole heterocycles have been synthesized and well characterised by Gabriel E. Buchel *et al.*[12] The antiproliferative activity of water-soluble compounds in the human cancer cell lines have been evaluated.

The results explained both the complexes have pronounced activity and the IC_{50} value of osmium complexes is significantly lower than ruthenium complexes.

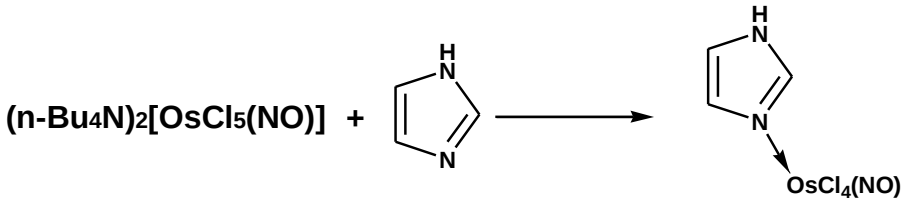

146 **147** **148**

Laihon Chang *et al.*,[13] have developed a bipyridine ligand having NNC donor system to metal ion and osmium complexes. The compound exhibits excellent photophysical properties and DFT studies also support the excitation of the compounds.

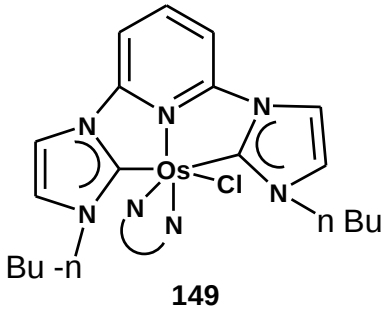

149

Osmium (III) complexes,[14] which are analogues of KP1019 were synthesised through electrochemical and chemical synthetic method and characterized by Paul. The complexes were subjected to cytotoxic activity. Compared with KP1019 and cisplatin, it exhibits significant activity.

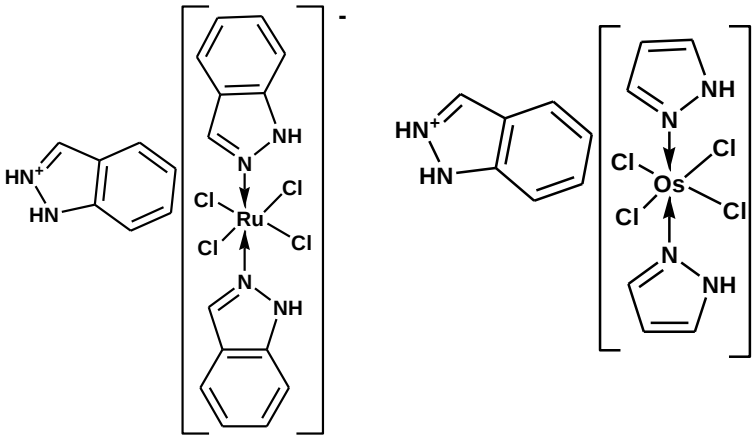

2 **150**

Patel *et al.*,[15] have designed and synthesised a reagent ie., osmium complex bearing phenanthroline system, which is obtained by the oxidation of complex using lead (IV) oxide. This reagent is used in the detection of acetaminophen in various pharmaceutical formulations and in urine. In urine, they have recovered 90% using selective method and successful detection of acetaminophen.

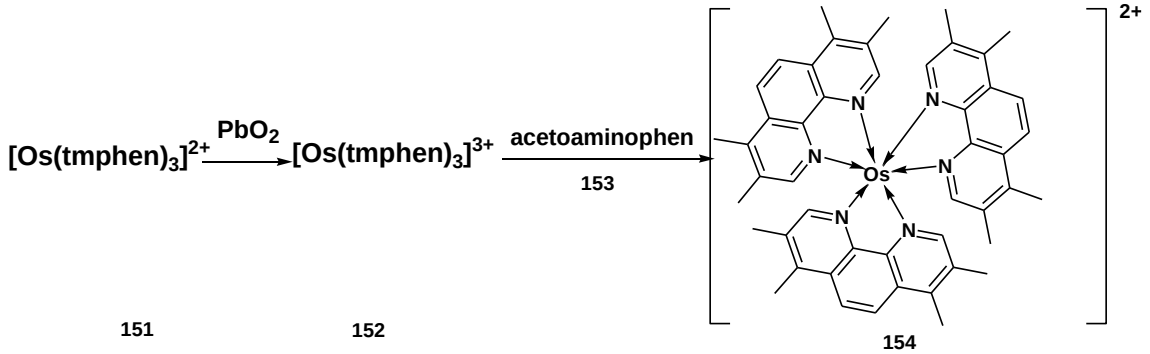

151 152 154

Poulami Pattanayak *et al.*,[16] have synthesised and characterized Os(II) **(157)** and Co(II) complexes containing NNO donor system of arylazo salicylidene system. The X-ray crystallographic studies confirmed the structure of complexes. The cyclic voltammteric studies showed that the system undergo one electron quasi reversible oxidative system. It is also used for catalytic hydrogenation of alcohols.

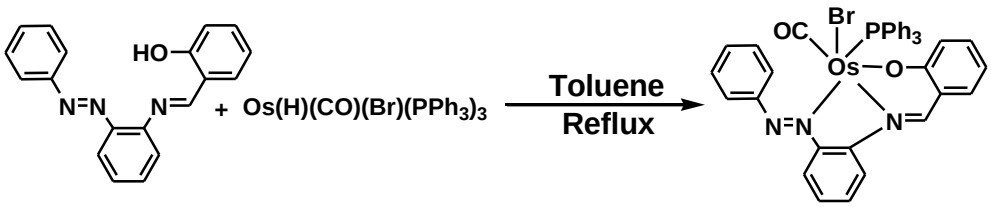

155 156 157

Soumik Mandal *et al.*,[17] have reported the synthesis and characterization of Ru(II) and Os(II) complexes having carbohydrate derived salen type of ligand. The complexes exhibited good photophysical properties and possesss redox behavior. Further the structure was confirmed by single crystal X-ray studies.

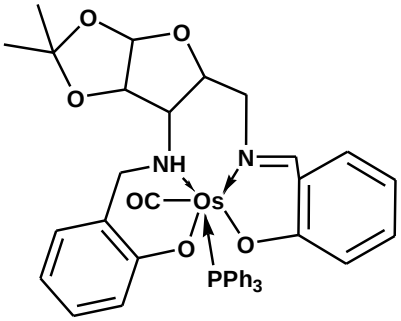

158

Roberto G. Alabau *et al.*,[18] have synthesized and characterized a novel homoleptic and heteroleptic NHC carbene containing bis(tridentate) osmium(II) complexes. The photophysical properties have been studied and the complexes exhibited blue-green emission with high quantum yields and reached maximum brightness.

Luis Casarrubios *et al.*,[19] carried out the reaction between 2-azetidinones and hexahydride osmium complex and synthesised NCC pincer complexes through the metal mediated degradation involving two CH bond activation followed by the rupture of C-N and C-C bonds of four membered ring.

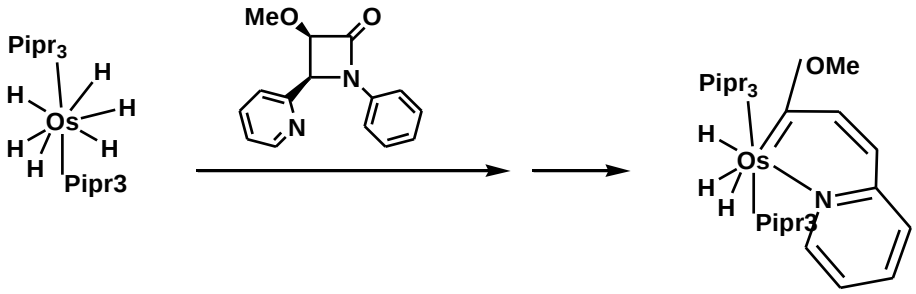

159 **160**

Maria L Buil *et al.*,[20] have effected a transformation of five membered hydride alkylidyne complex to 16 VE alkylidyne complex. This structure was confirmed by X-ray crystallography. Further, the complex was subjected to oxidative addition of alkynes and leads to five coordinated alkylidene osmium complexes.

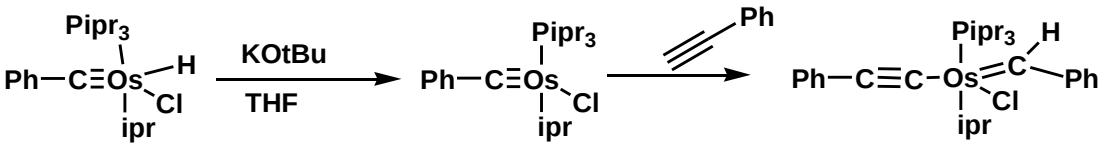

161 **162** **163**

The X ray crystallography of a series of arene osmium complexes having ethacrynic acid was reported by Gabriele Agonigi *et al.*[21] The complexes act as potential inhibitor of glutathione-S-transferases. The antiproliferative activity of the complexes were screened and results found that the activity is equal to ruthenium (III) congeners.

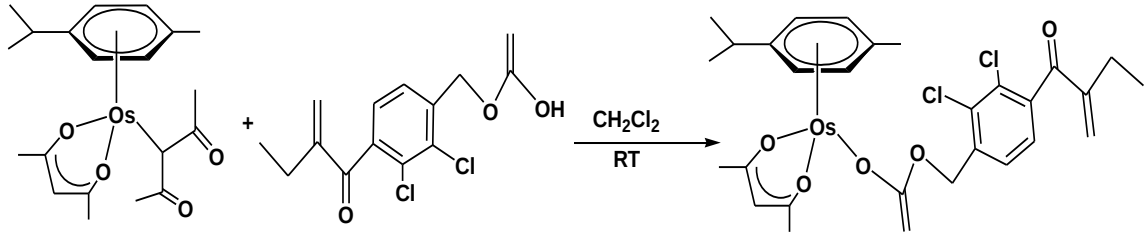

164 **165** **166**

Maria S. Novak *et al.*,[22] have synthesized the ruthenium- and osmium nitrosyl complexes with azole heterocycles, studied their cytotoxicity and possible interactions with DNA. Apoptosis induction, changes of mitochondrial transmembrane potential and possible formation of reactive oxygen species were investigated as indicators of NO-mediated damage by flow cytometry. The results proposed that complexes of ruthenium and osmium having azole heterocycles have marked cytotoxic potency against cancer cell lines.

Ludovic favereau *et al.*,[23] designed a strategy for artificial photosynthesis using Ru (II)-Os (III) dyads containing bipyridine system. TiO_2 nano crystals were used as electrodes for the process. The photophysical studies confirmed the electron transfer from Ru (II) to Os (III) represented as

MLCT to LMCT and Ru (II) $\longrightarrow$ Os (III) quenched by this process.

Gabriel E. Büchel *et al.*,[24] reported the synthesis and crystal structure of $[Os^{IV}Cl_4(Hazole)_2]$, where H-azole = indazole, pyrazole,benzimidazole, and imidazole. Electrochemical and chemical one-electron reduction of complex gave osmium(III) species isolated as tetrabutylammonium and sodium salts respectively. X-band EPR spectra of the complexes showed broad lines with a rhombic g-tensor signifying the low-spin $5d^5$ configuration. The compounds were evaluated for antiprolliferative activity and exhibited pronounced activity.

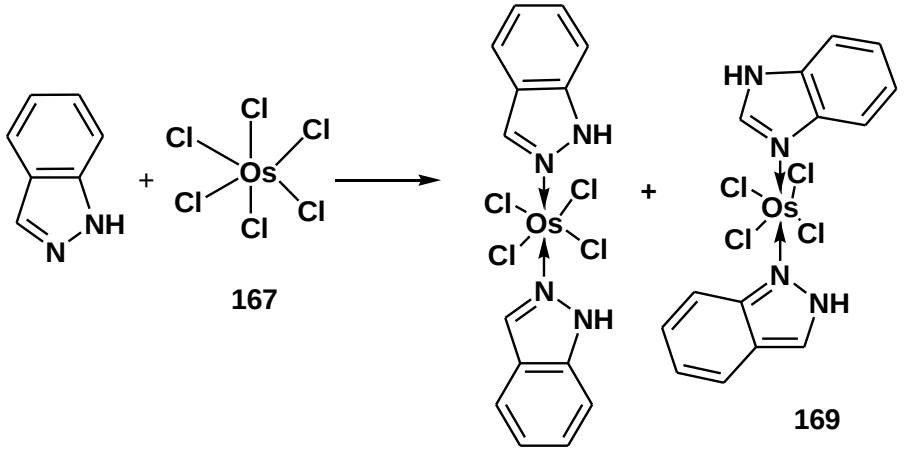

167 **168** **169**

A series of Os(III) and Os(II) complexes bearing hexadenate chelating system was synthesised and characterized by Hideki *et al.*[25] Due to the chelation, the octahedral geometry becomes distorted and labile towards the substitution reaction, forming the anionic bound Os(III) complexes.

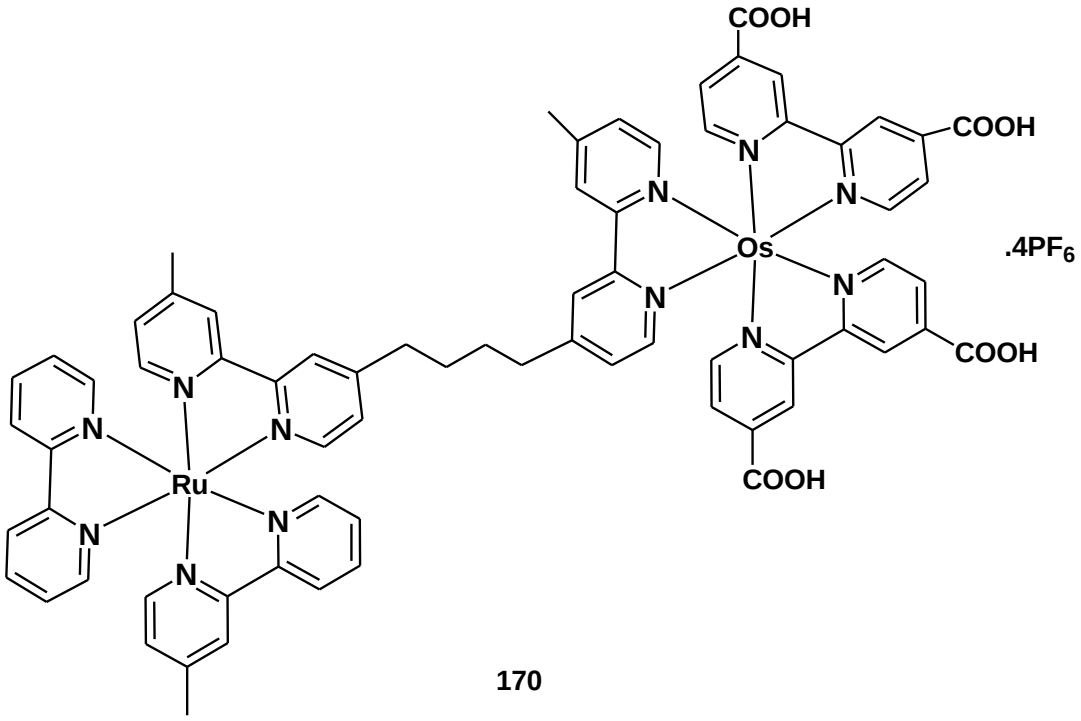

170

4.2. Results and Discussion

Osmium complexes can coordinate to ligands in a chelating mode which forms pincer compounds, the pincer complexes possess the ability of catalytic transformations and in materials applications.[26] They can be used as intermediates for many organic reactions. Osmium has variable oxidation states Os(II), Os(III) and Os(IV) and even higher. This plays an important role in biological redox regulation within cancer cells.[27]

Os(II/III) analogues of known Ru(II/III) complexes including Os-RAPTA-C, Os-RM175 and Os-NAMI-A, Os(III)pyridine derivatives have been designed as anticancer agents.

4.2.1. Synthesis of Os(III) complex (18a)

The reaction was carried out by taking equal moles of $OsCl_3.3H_2O$ and 4-methyl-2-(salicylidenehydrazino)quinoline **(11a)** in ethanol and heated under reflux for 8 h in a water bath. After the periodic monitoring of the reaction mixture, the product obtained was confirmed by TLC. The reaction mixture was cooled and the solid formed was washed and recrystallized from ethanol/chloroform mixture.

M.pt > 200 ^oC yield -0.43 g(53%)

Molar conductivity of the complex **18a** was measured in DMSO solution of 10^{-3} M. The calculated molar conductance is of 9 $mho.cm^2.mol^{-1}$. The low value indicates the non-electrolytic nature of the complex.

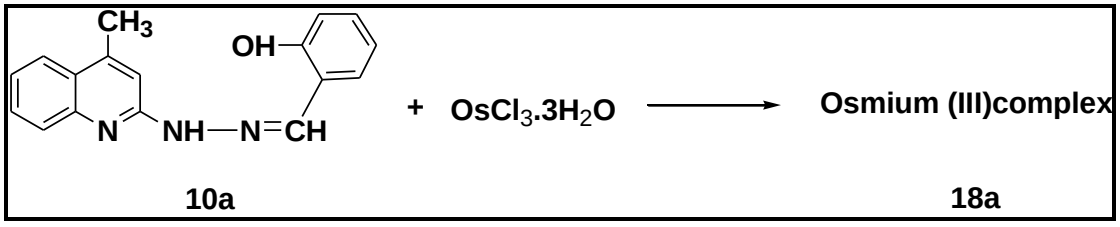

Scheme 10

IR spectrum (υ_{max} in cm^{-1}) (fig **132):** Compound **18a** exhibited a broad peak at 3347 cm^{-1} corresponding to the presence of water molecules and there is no absorption noticed in the range of 2900 cm^{-1}- 3000 cm^{-1}. So it is clear that there is no –NH bond in the complex formed and no shift in stretching frequency in –C=N, which might lead to the conclusion that NNO coordination mode of the hydrazinoquinoline Schiff base.

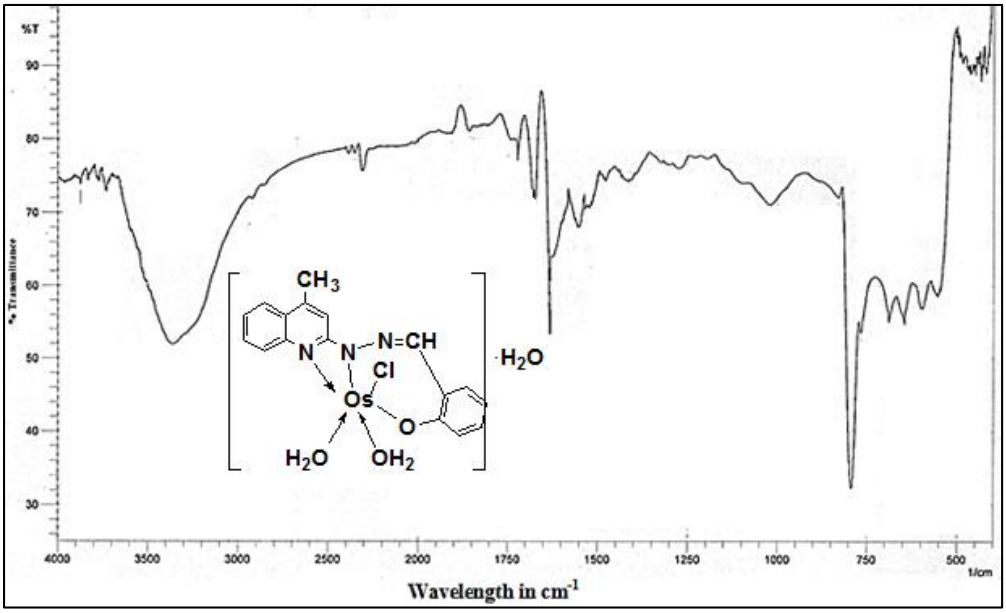

Fig 132 - IR spectrum of osmium complex 18a

^{1}H-NMR spectrum of the complex **18a (fig 133)** shows 9 proton multiplet at 7.9-7.3 ppm (ie) 8 for aromatic protons and one for azomethine protons and 4.1 ppm for hydroxy protons and 2.4 ppm for methyl protons.

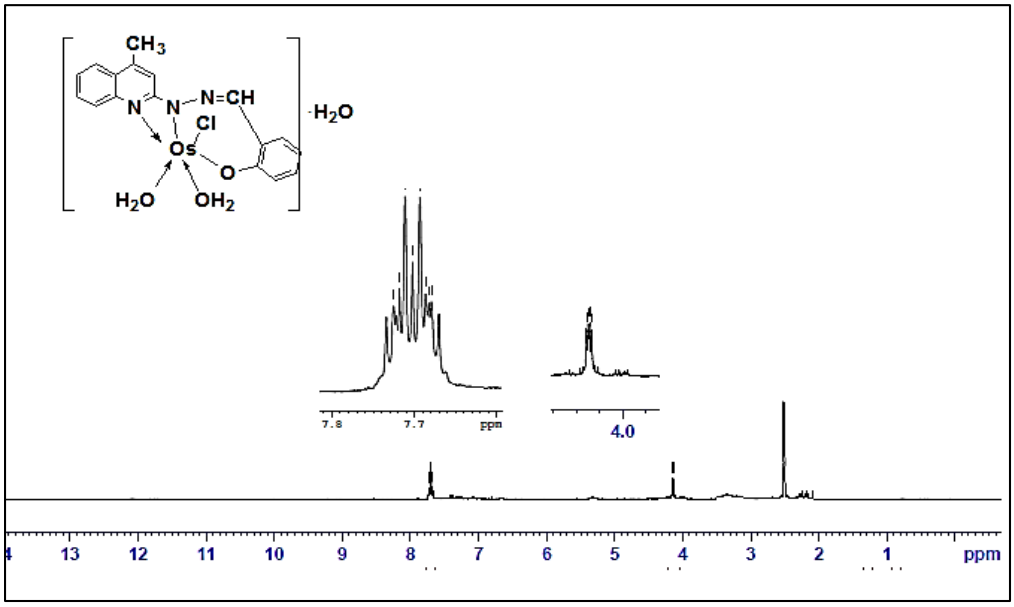

Fig 133 - ^{1}H NMR spectrum of osmium complex 18a

The disappearance of peak at 10.8 ppm and 9.9 ppm for –NH and –OH of the ligand **(11a)** respectively show the coordination to metal through –NH and –OH.

The **UV spectrum** of complex (**18a) (fig 134)** exhibited bands at 205 nm, 390 nm and 580 nm.

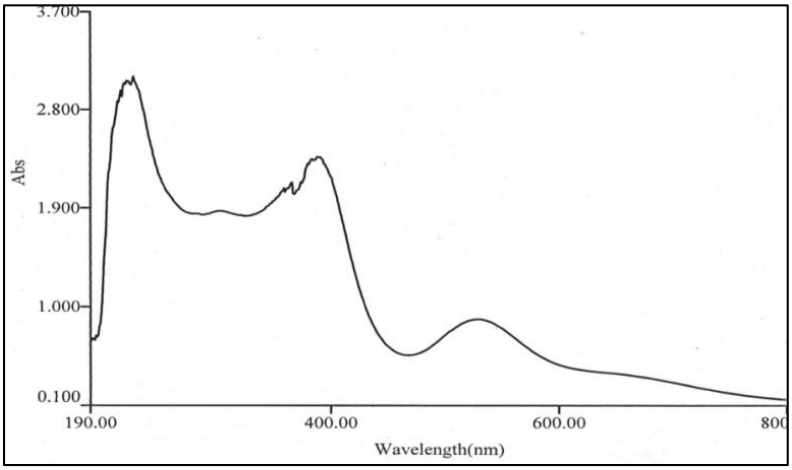

Fig 134 - UV spectrum of osmium complex 18a

The band at 205 nm is assigned to intra ligand transitions. The band at 390nm is due to ligand metal transition ie., transfer of electrons from ligand to metal orbital. The less intense weak band at 560 nm is due to the MLCT transitions.

The **thermogravimetric studies** of the complex **18a** was carried at the heating rate of 10 ºC min^{-1} under nitrogen atmosphere and weight loss as measured from the ambient temperature upto 1000 ºC

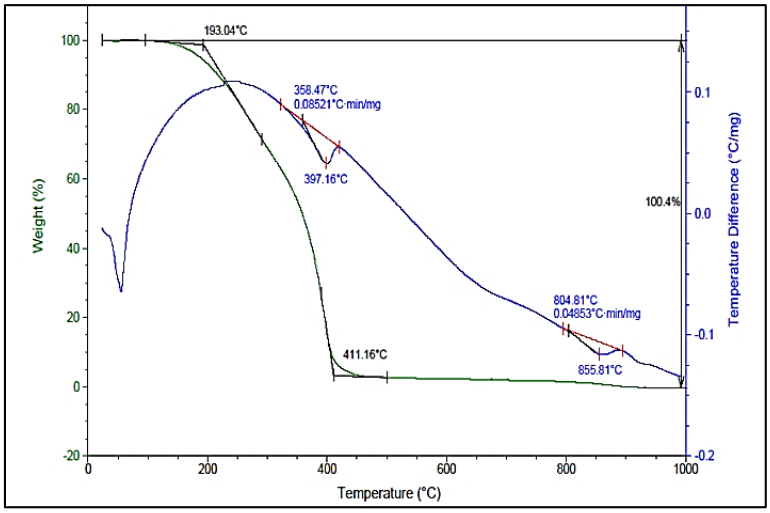

Fig 135 - TGA and DSC curve of osmium complex 18a

The **TGA Fig(135)** metal complex**(18a)** shows three stage decomposition.

The first decomposition was observed at the temperature range 110 ºC. The percentage weight loss (3%) in this range corresponds to the loss of one lattice water molecule. Next decomposition is at the temperature range 210 ºC, (12%) loss indicates the loss of two coordinated water molecules and one chlorine atom. Finally there is gradual decrease in mass loss with increase in temperature range of 400 - 1000 ºC corresponding to the ligand decomposition and leaving the metal residue.

The residues subsequently fragment through several exothermic process and shown by the DSC curve.

Hence from the spectral and analytical data, it was confirmed that the ligand **11a** is coordinated to the osmium (III) complex in the plausible type **11a(iii)** , the structure of the metal complex (**18a)** obtained is

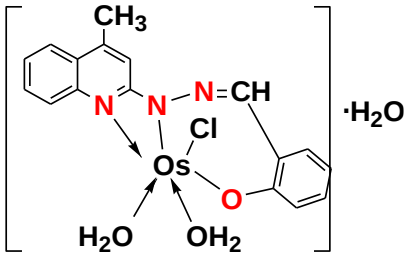

18a

Therefore the ligand coordinated to metal complexes through NNO donor mode and it is tridenate in nature.

The same methodology was extended to derivatives and found that all the spectral data are similar and therefore the structure of metal complexes **18(b-d) in chart VII.**

Chart VII

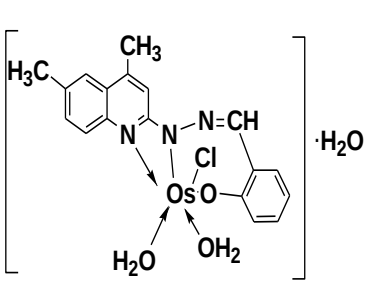

18b

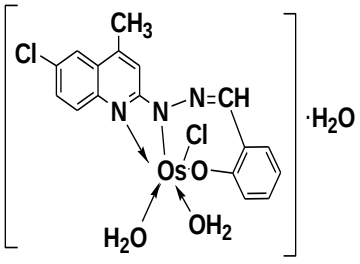

18c

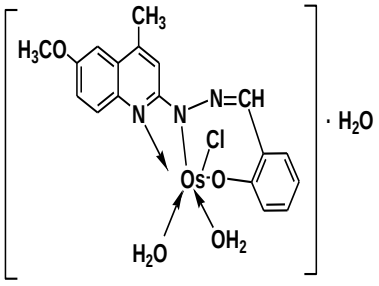

18d

4.2.1. Synthesis of Os (III) complex (19a)

After achieving hydrazinoquinoline, we extended the synthesis of Os(III) complexes with 4-methyl-2-(salicylidenethiosemicarbazino)quinoline**(13a).** Equal moles of $OsCl_3.3H_2O$ and ligand **13a** in ethanol were refluxed for 15 h and after usual workup procedure. Complex **19a** was obtained as a dark blue crystalline solid. M.pt >200°C with an yield of 0.42 g (52%).

The conductance of the complex **19a** was measured in DMSO solution of 10^{-3}M using conductivity bridge. From this value, molar conductance was calculated and found 15 mho cm^2 mol^{-1}, which clearly indicates that it is non electrolyte.

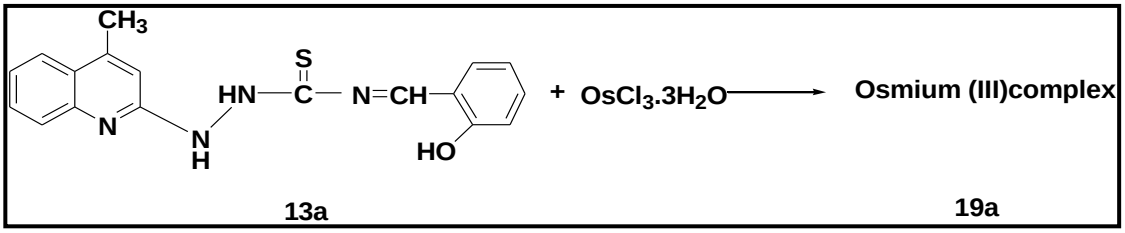

Scheme 11

IR spectrum (υ_{max} in cm^{-1}) **(fig 136):** Complex **19a** exhibited bands 3383(OH), 3050(NH), 3085(NH), 1627(-C=N), 1520(-C=N), 1416(-C=S), 1091(-C-O), 690 (M-Cl), 437(M-O) respectively.

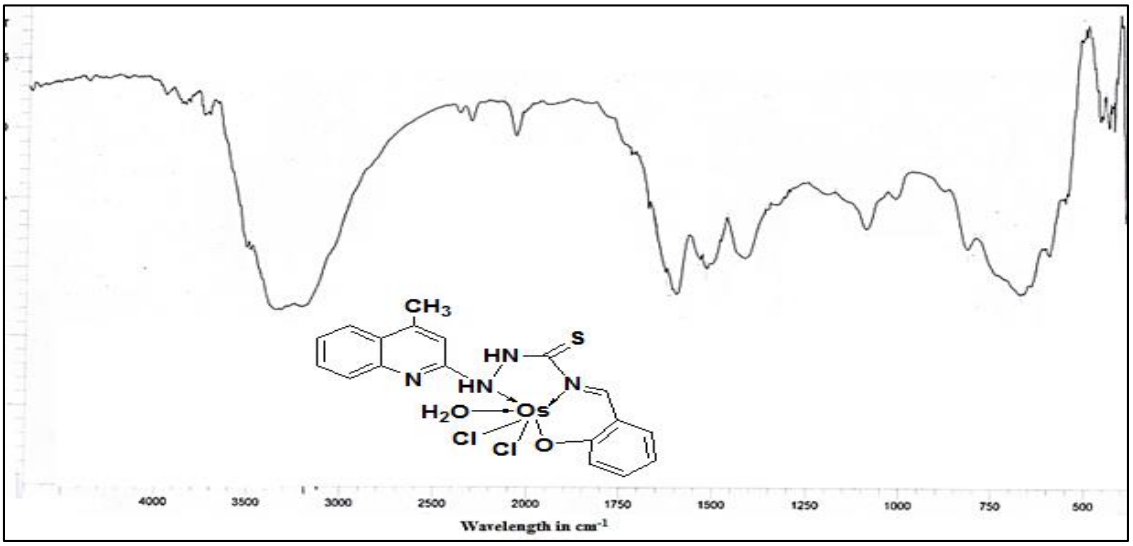

Fig 136 - IR spectrum of osmium complex 19a

The shift in the IR spectral value when compared with corresponding ligand **13a (fig 16)** shows that the coordination takes place through NNO mode. Further the value obtained for –C=N of quinoline ring indicates that –N of quinoline is not involved in the coordination.

^{1}H-NMR spectrum (DMSO) (δ in ppm) **(**fig **137)**: A shift in a signal from δ 10.2 of –NH of ligand **13a (fig 17)** to δ 9.8 ppm in the complex **(19a)** towards downfield indicated that the electron density around–NH group is donated to the metal ion. Therefore, it is more deshielded and complete disappearance of phenolic –OH group of the ligand (**13a**) was noted. The appearance of new peak at δ 5.8 ppm confirmed the presence of coordinated water. A singlet signal at δ 2.4 ppm for three methyl protons and multiplet appeared at δ 6.3- δ 8.2 ppm for 9 aromatic and one azomethine protons.

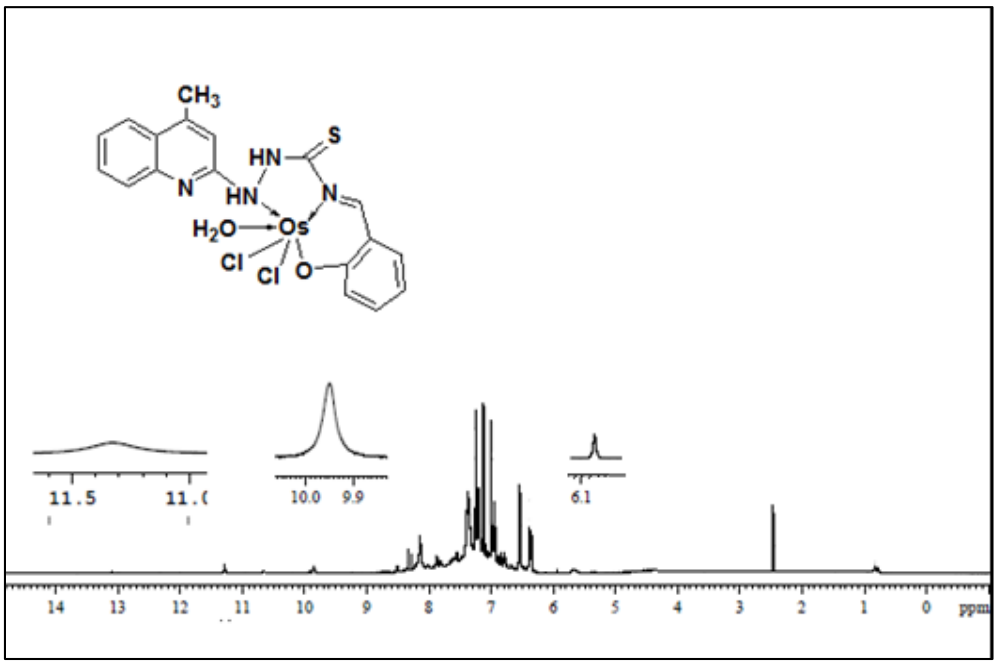

Fig 137 - ^{1}H-NMR spectrum of osmium complex 19a

The thermal analysis supported the formation of metal complex **19a (fig 138).** The TG curve shows two decomposition points.

The first stage decomposition was noticed at the temperature range 240 ºC with percentage weight loss (14.4 %) indicating the loss of two coordinated water molecules and one chlorine atom. Then weight loss of 20% at the temperature of 380 ºC indicates the cleavage of phenoxy ion. The gradual decrease in weight upto 520 ºC with the

elimination of two nitrogen and one sulphur resulting in loss of 14.2%. After this point, linear decrease and complete decomposition was noticed with the metal residue corresponding to 20% mass residue.

The residue subsequently fragments through two exothermic process and was shown by the DSC curve.

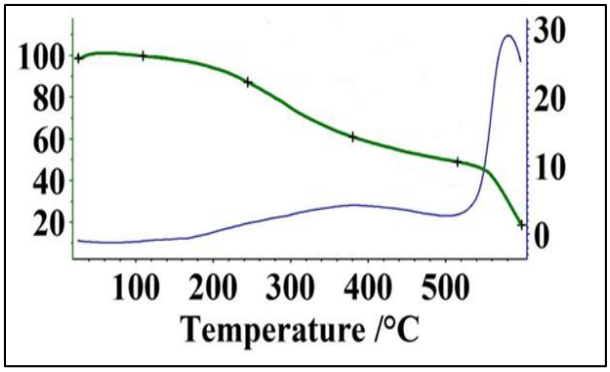

Fig 138 - TGA and DSC curve of osmium complex 19a

The XRD curve of the complex 18a was shown in **fig 139** and lattice parameters were found to be a = 9.0543, b = 12.8534, c = 15.0541 and α= 90 º β= 91.27 º, γ = 90º and belongs to monoclinic system using fullprof suite program.

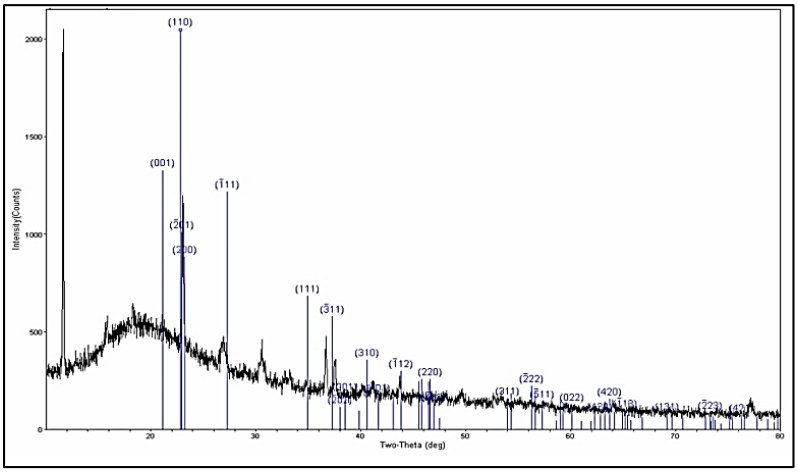

Fig 139 - XRD pattern of osmium (III) complex 18a

From these spectral and analytical results, we concluded that ligand **13a** is coordinated to metal through the NNO sites and form stable chelated system.

The structure of complex **19a** is

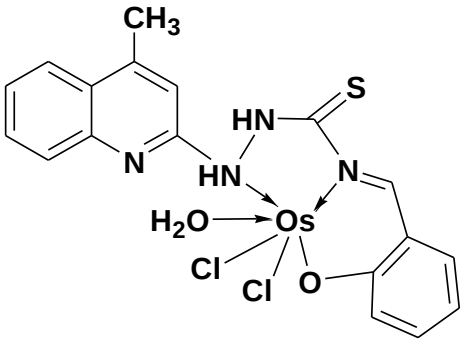

Similar procedure was followed to obtain the derivatives **19(b-d)** and they were characterized by spectral studies. The results obtained are in the range similar to those of **19a**. The structures of complexes 19 (b-d) are as represented in **chart VIII.**

Chart VIII

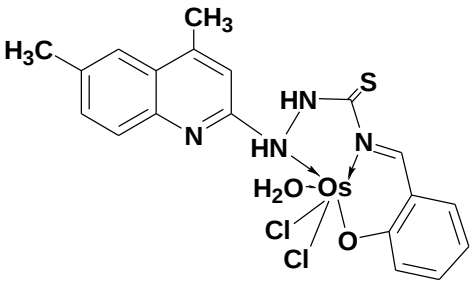

19b

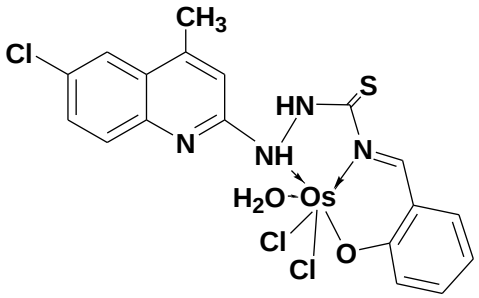

19c

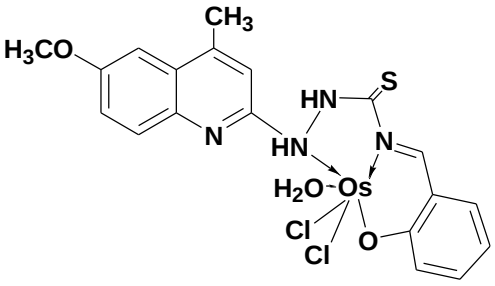

19d

This is further evidenced by DFT studies.

The optimized geometry of the complex **18a** and **19a** was found.

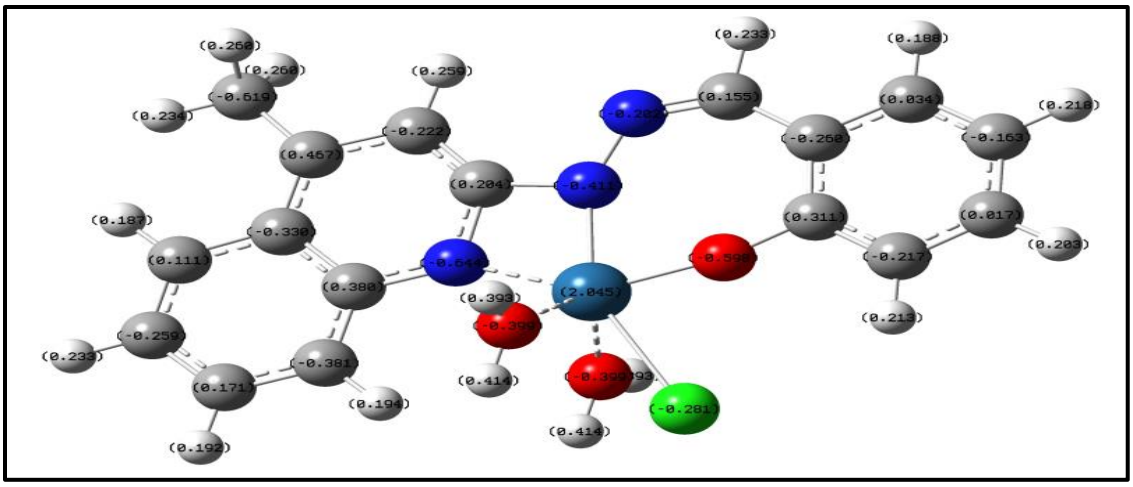

Fig 140- Optimized geometry of osmium complex 18a

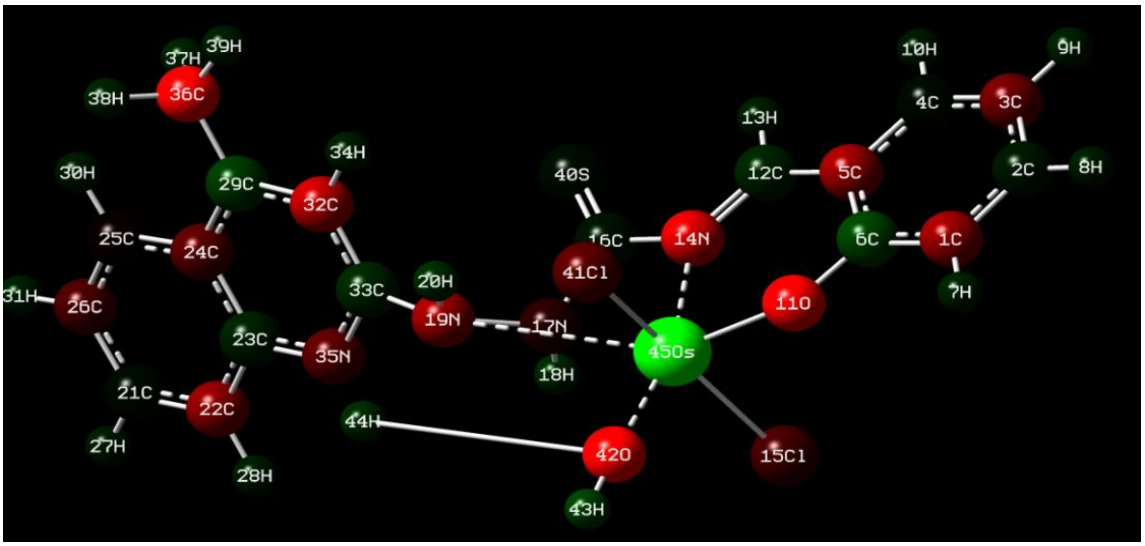

Fig 141- Optimized geometry of osmium complex 19a

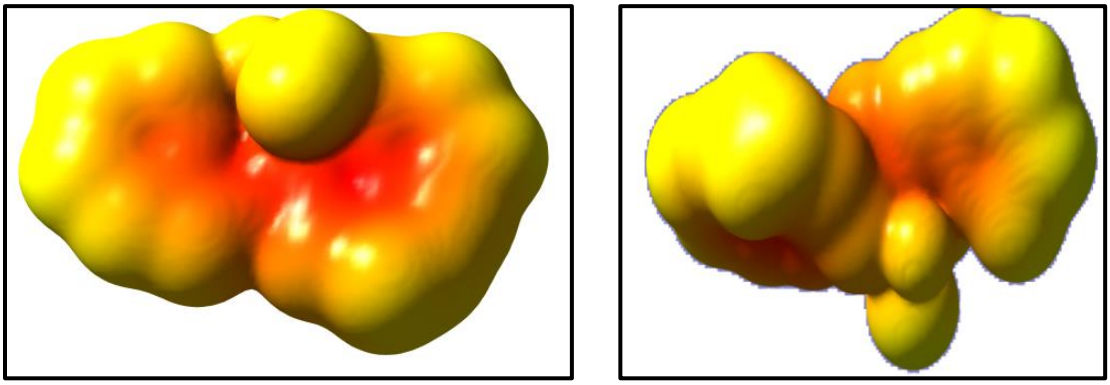

Fig 142 a & b MEP diagram of osmium complex 18a and 19a

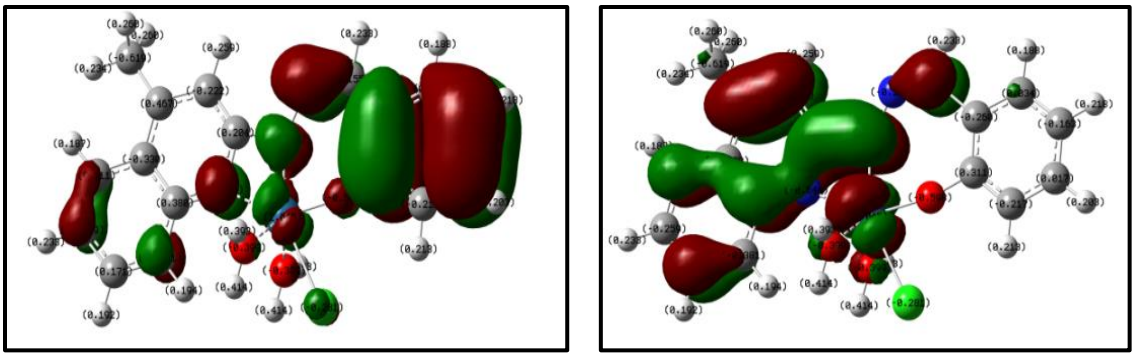

Fig 143- HOMO and LUMO structures of complex 18a

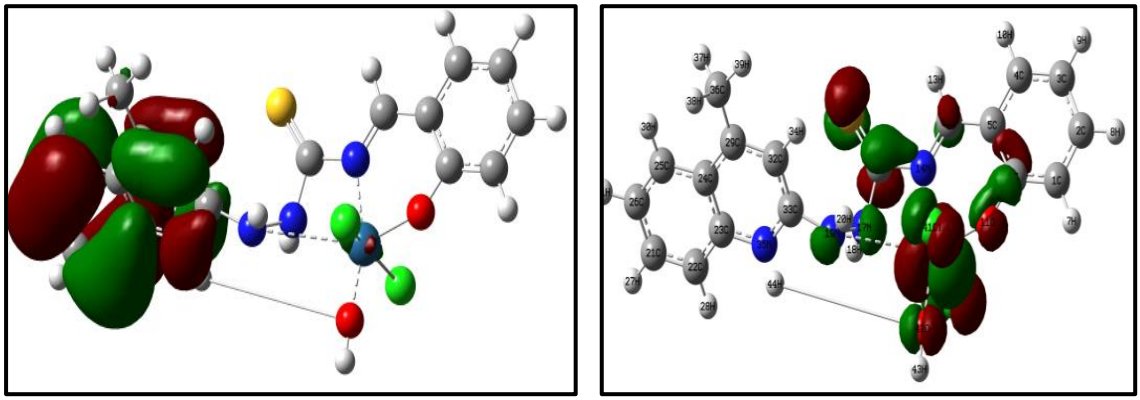

Fig 144 - HOMO and LUMO structures of complex 19a

The theoretical & experimental results were well coincided and are well in line with the Mulliken charge and energy gap of the system.

Table 13: Comparison of Mulliken charges of metal complexes 18a & **19a and ligands 11a** and **13a**

Atom 11a	**Mulliken charge**	**Atom 18a**	**Mulliken charge**	**Atom 13a**	**Mulliken charge**	**Atom 19a**	**Mulliken Charge**
15N	-0.487	15N	-0.411	20N	-0.490	19N	-0.336
30O	-0.559	31O	-0.598	25N	-0.545	14N	-0.485
32N	-0.655	14N	-0.644	38O	-0.556	11O	-0.590

Table 14: Energy parameters of complexes 18a & **19a**

In eV	**18a**	**18b**	**18c**	**18d**	**19a**	**19b**	**19c**	**19d**
HOMO	17.92	17.80	17.47	17.05	17.47	17.77	17.41	17.03
LUMO	12.47	12.38	12.52	12.38	11.69	12.19	12.31	12.25
ΔE	5.45	5.42	4.95	4.67	5.78	5.58	5.10	4.78

4.3. Experimental

General Procedure for the Synthesis of Osmium (III) Complexes

4.3.1. Preparation of new osmium (III) hydrazinoquinoline Complexes: 18b-18d

To a stirred solution of osmium trichloride trihydrate($OsCl_3.3H_2O$) in 40mL ethanol, 4-methyl-2-(salicylidene hydrazino) substituted quinoline (11a-11d) was added and the reaction mixture was under heated reflux for 8 h and completion of the reaction was monitored with TLC. Dark coloured crystals obtained were separated, washed with ethanol and dried under vacuum.

4.3.1.1. Preparation of osmium(III)complex 18b

Osmium trichloride trihydrate	**:**	0.5 g (1.43 mmol)
4,6-dimethyl-2-(salicylidene hydrazino)quinoline	**:**	0.42 g (1.43 mmol)
Ethanol	**:**	40-50 mL
Color	**:**	Blue
Yield	**:**	0.42 g (54%).

M.Pt >300 ^{o} C Anal. calcd for $C_{18}H_{19}N_3O_3ClOs$: C, 40.58 ; H, 3.57 ; N, 7.89 %, Found: C, 41.8 ; H, 4.6 ; N, 8.5 %.

IR (cm^{-1}) (υ_{max}) (fig 145) Compound **18b:** 3300 (-OH), 1605(-CN), 1150 (-CO).

^{1}H NMR (DMSO) (ppm) (fig 146) Compound **18b:** δ7.8 to 6.9, (m,aromatic and azomethine protons), δ1.9 (–CH_3), δ2.4 (–CH_3).

4.3.1.2. Preparation of osmium(III)complex 18c

Osmium trichloride trihydrate	**:**	0.5 g (1.43 mmol)
4-methyl-6-chloro-2-(salicylidenehydrazino)quinoline	**:**	0.44 g (1.43 mmol)
Ethanol	**:**	40-50 mL
Color	**:**	Blue
Yield	**:**	0.38 g (47%)

M.Pt >300 ºC Anal. calcd for $C_{17}H_{16}N_3O_3Cl_2Os$: C, 36.94 ; H, 2.89 ; N, 7.60 %, Found: C, 35.4 ; H, 3.9 ; N, 8.1 %.

IR (cm^{-1}) (υ_{max}) (fig 147) Compound **18c:** 3291 (-OH), 1629(-CN), 1056 (-CO).

4.3.1.3. Preparation of osmium(III)complex 18d

Osmium trichloride trihydrate	**:**	0.5 g (1.43 mmol)
4-methyl-6-methoxy-2-(salicylidenehydrazino)quinoline	**:**	0.44 g (1.43 mmol)
Ethanol	**:**	40-50 mL
Color	**:**	Blue
Yield	**:**	0.35 g (43%)

M.Pt >300 ºC Anal. calcd for $C_{18}H_{19}N_3O_4ClOs$: C, 39.41 ; H, 3.46 ; N, 7.66 %, Found: C, 41.1 ; H, 3.9 ; N, 8.9 %.

IR (cm^{-1}) (υ_{max}) (fig 148) Compound **18d:** 3300 (-OH), 1605(-CN), 1150 (-CO).

4.3.2. Preparation of new osmium (III) thiosemicarbazinoquinoline complex: 19(b-d)

Osmium trichloride trihydrate ($OsCl_3.3H_2O$) and 4-methyl-2-(salicylidene thiosemicarbazino) substituted quinoline was taken in an equal mole ratio and completely dissolved in 40mL of ethanol and then the reaction mixture was heated under reflux in a water bath for 12 - 15 h. The solid product obtained were filtered, washed with ethanol and dried under vacuum.

4.3.2.1. Preparation of osmium(III)complex 19b

Osmium trichloride trihydrate	**:**	0.5 g (1.43 mmol)
4,6-dimethyl-2-(salicylidenethiosemicarbazino) quinoline	**:**	0.52 g (1.43 mmol)
Ethanol	**:**	40-50 mL
Color	**:**	yellow
Yield	**:**	0.45 g (53%).

Mp > 300 ºC, Anal. calcd for $C_{19}H_{19}N_4O_2SCl_2Os$: C, 36.36 ; H, 3.03 ; N, 8.93; S, 5.10 %, Found: C, 37.8 ; H, 3.5 ; N, 8.1; S, 6.5 %.

IR (cm^{-1}) (υ_{max}) (fig 149) Compound **19b:** 3226(OH), 3014(NH), 2840(NH), 1656 (-C=N), 1437(-C=N), 1227(-C=S), 1198(-C-O), 678 (M-Cl).

^{1}H NMR (DMSO) (ppm) (fig 150) Compound **19b:** δ11.3 (–NH), δ9.8(–NH), δ 8.0 to 6.3, aromatic protons gives multiplet signals, δ 2.3 (–CH_3), δ 2.3 (–CH_3), δ 6.1 (-OH).

4.3.2.2. Preparation of osmium(III)complex 19c

Osmium trichloride trihydrate	**:**	0.5 g (1.43 mmol)
4-methyl-6-chloro-2-(salicylidenethiosemicarbazino) quinoline	**:**	0.55 g (1.43 mmol)
Ethanol	**:**	40-50 mL
Color	**:**	Reddish brown
Yield	**:**	0.41 g(47%).

Mp > 300 ºC, Anal. calcd for $C_{18}H_{16}N_4O_2SCl_3Os$: C, 33.38 ; H, 2.47 ; N, 8.65; S, 4.94 %, Found: C, 35.6 ; H, 3.6 ; N, 9.5; S, 6.1 %.

IR (cm^{-1}) (υ_{max}) (fig 151) Compound **19c:** 3100(OH), 3009(NH), 2828(NH), 1677 (-C=N), 1588(-C=N), 1278(-C=S), 1160(-C-O), 665 (M-Cl).

4.3.2.3. Preparation of osmium(III)complex 19d

Osmium trichloride trihydrate	**:**	0.5 g (1.43 mmol)
4-methyl-6-methoxy-2-(salicylidenethiosemicarbazino)quinoline	**:**	0.54 g (1.43 mmol)
Ethanol	**:**	40-50 mL
Color	**:**	Brown
Yield	**:**	0.38 g (43%)

Mp > 300 ºC, Anal. calcd for $C_{19}H_{19}N_4O_3SCl_2Os$: C, 35.45 ; H, 2.95 ; N, 8.70; S, 4.97 %, Found: C, 36.8 ; H, 4.6 ; N, 7.2; S, 6.01 %.

IR (cm^{-1}) (υ_{max}) (fig 152) Compound **19d:** 3350(OH), 3050(NH), 2975(NH), 1594 (-C=N), 1350(-C=S), 1090(-C-O), 698 (M-Cl), 336 (M-O).

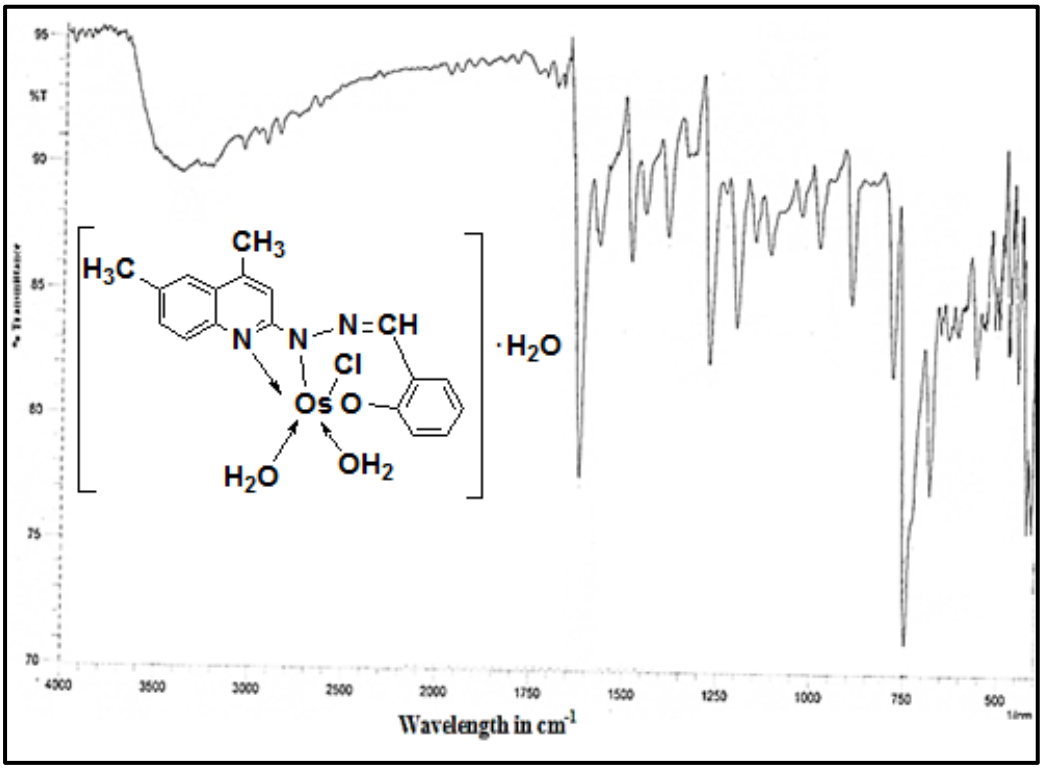

Fig 145 - IR spectrum of osmium (III) complex 18b

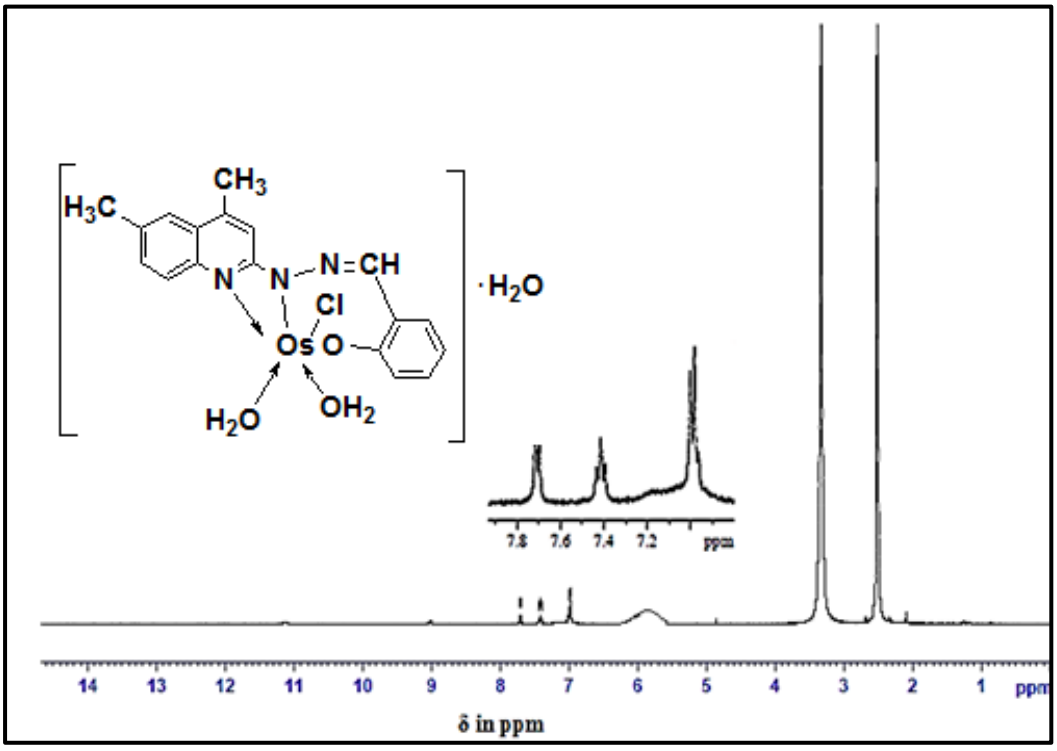

Fig 146 – ^{1}H-NMR spectrum of osmium (III) complex 18b

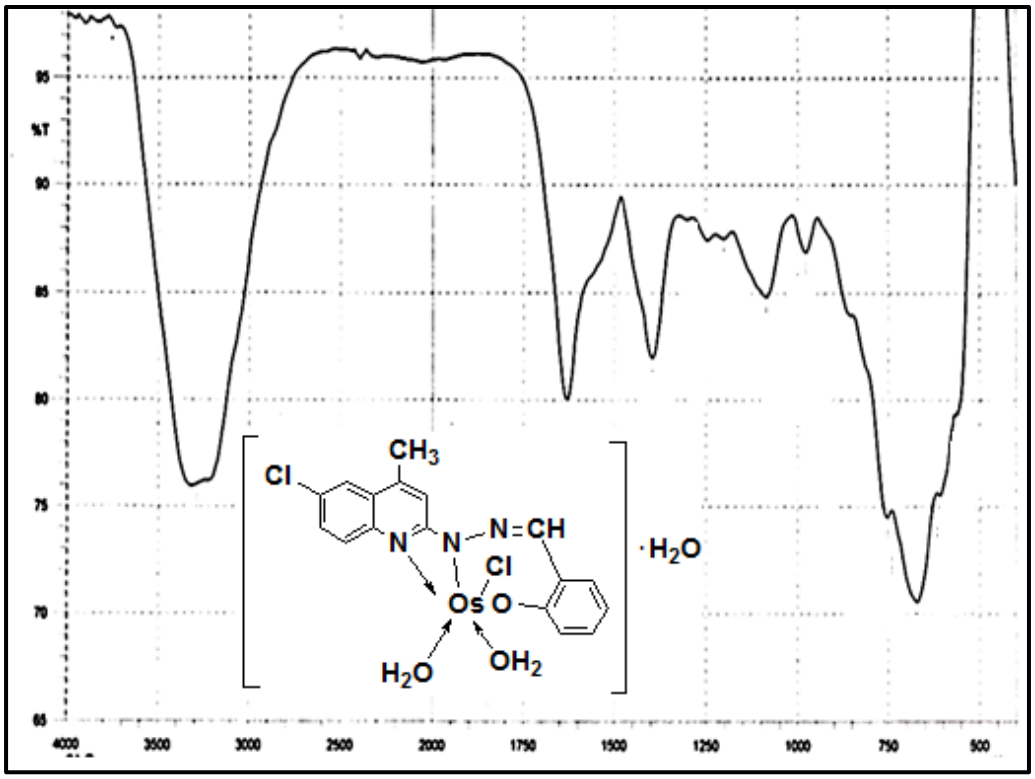

Fig 147 - IR spectrum of osmium (III) complex 18c

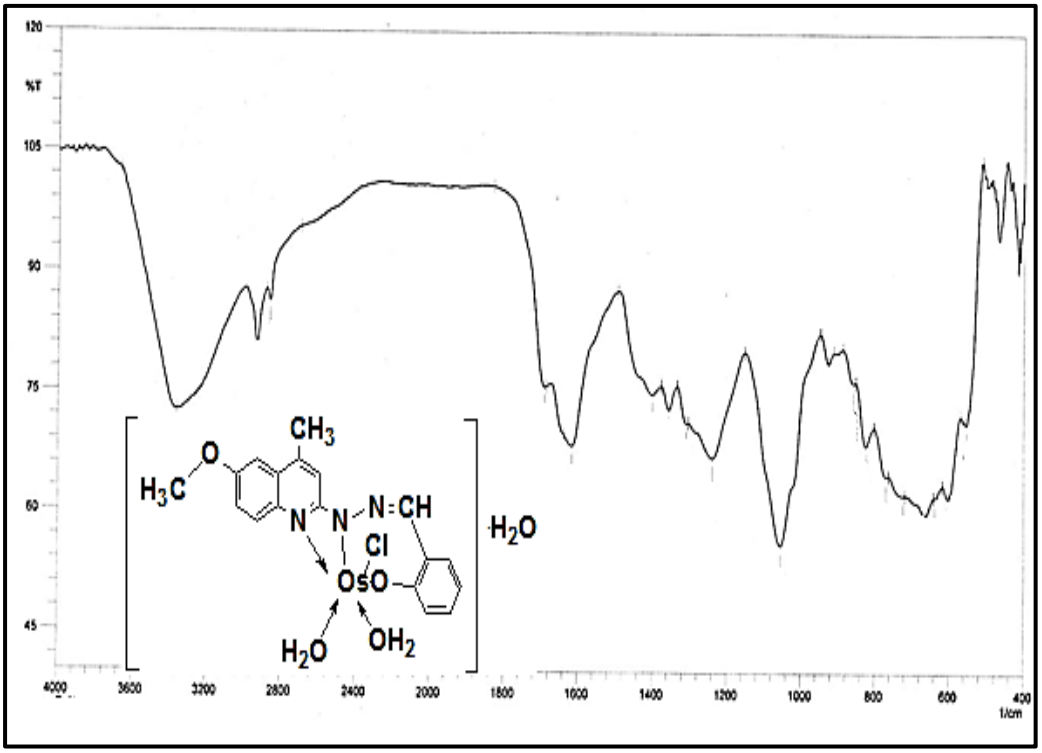

Fig 148 - IR spectrum of osmium (III) complex 18d

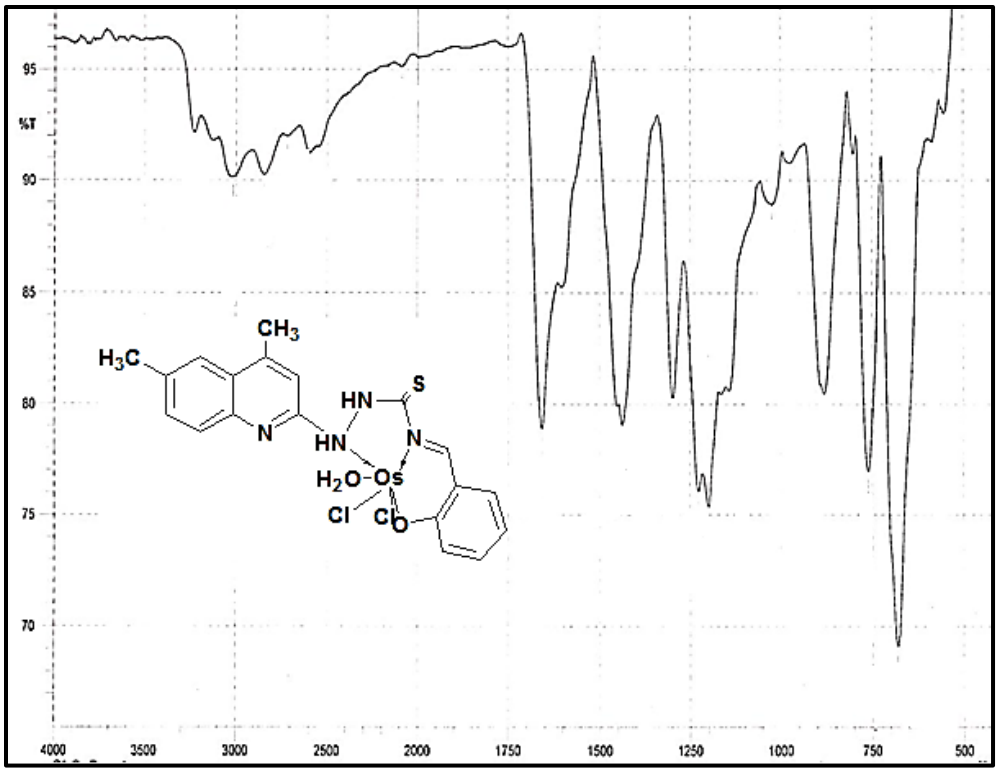

Fig 149 - IR spectrum of osmium (III) complex 19b

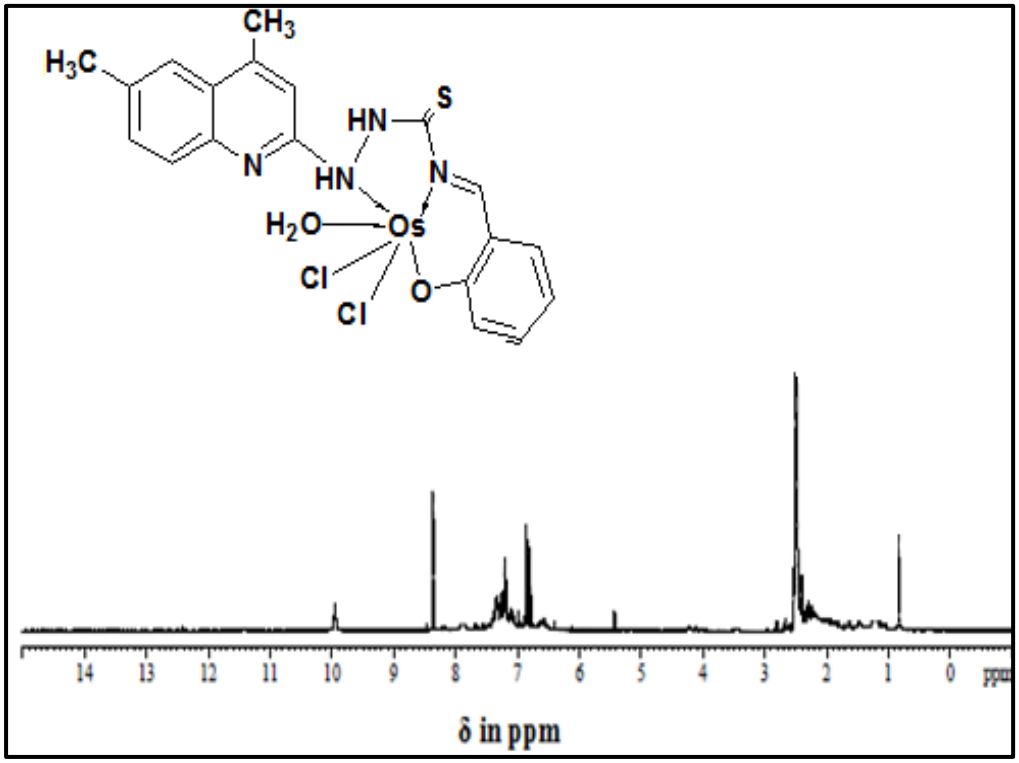

Fig 150 - ^{1}H-NMR spectrum of osmium (III) complex 19b

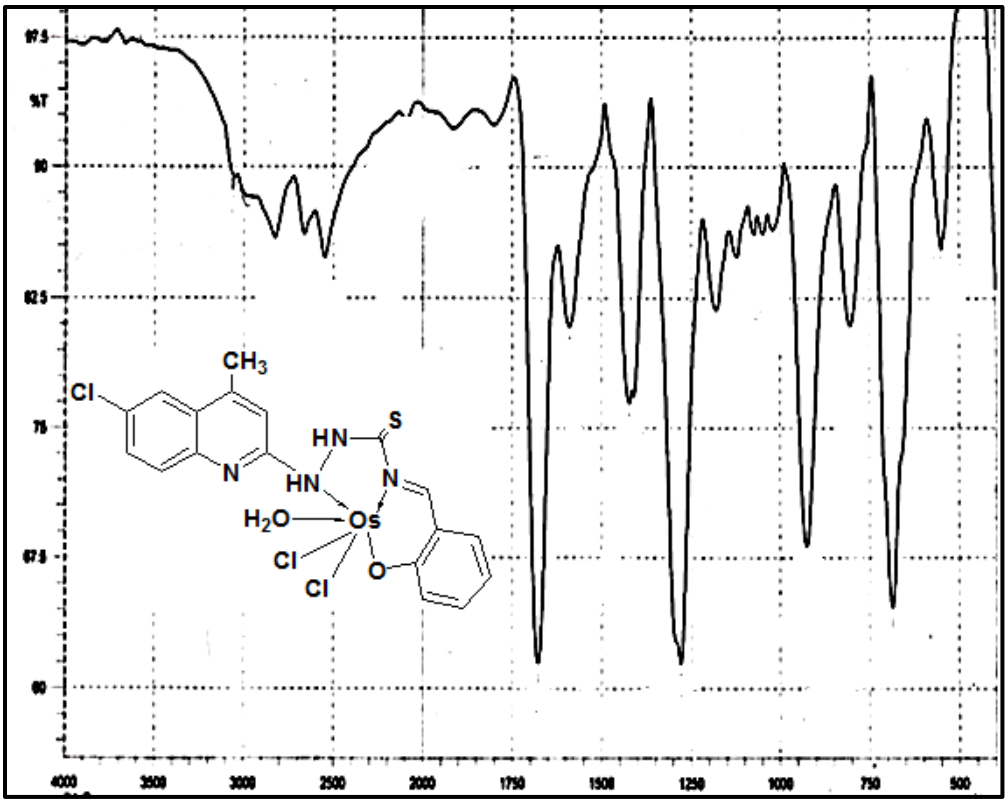

Fig 151 - IR spectrum of osmium (III) complex 19c

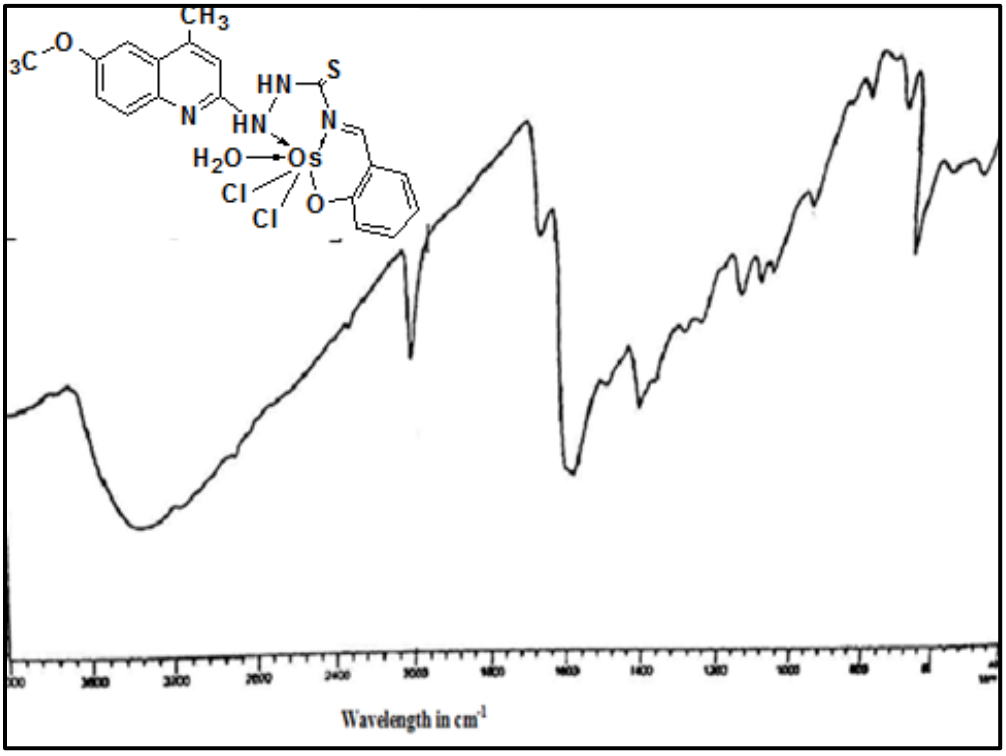

Fig 152 - IR spectrum of osmium (III) complex 19d

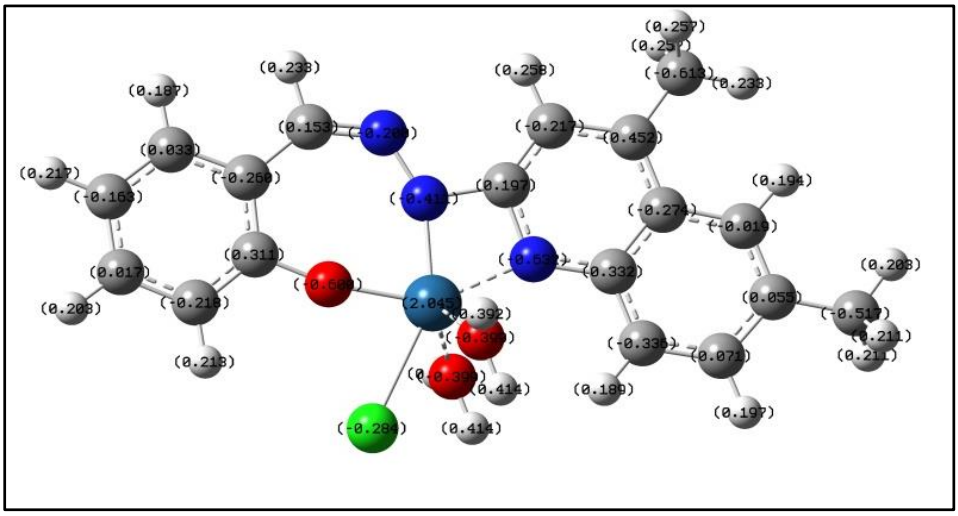

Fig 153 – Optimised geometry of osmium complex 18b

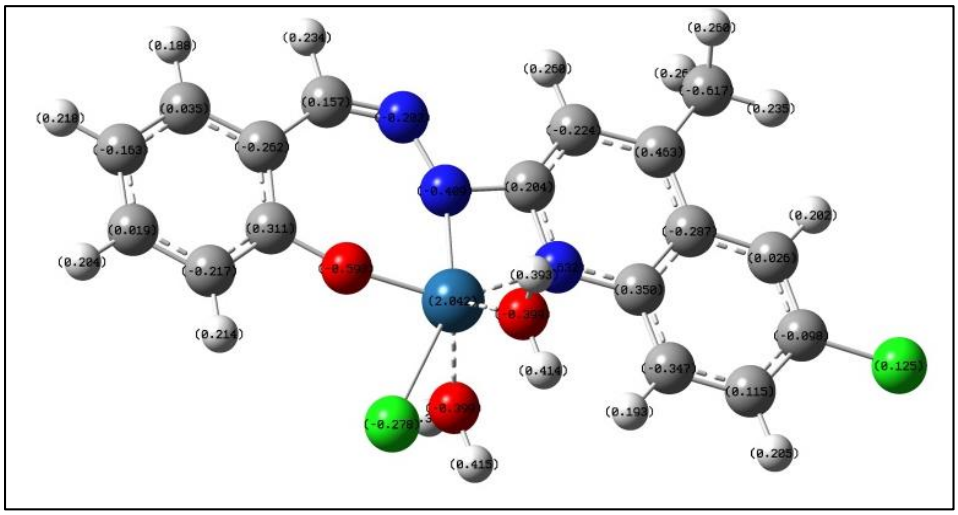

Fig 154 – Optimised geometry of osmium complex 18c

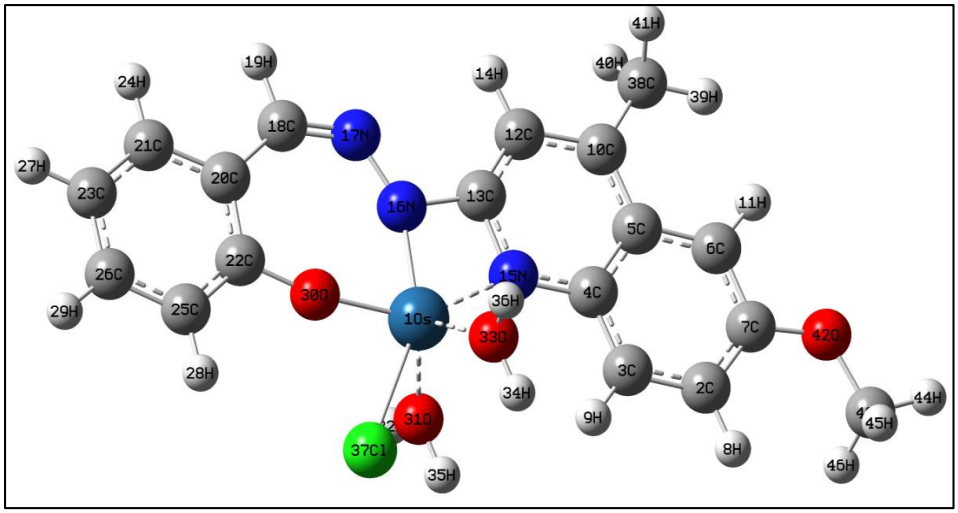

Fig 155– Optimised geometry of osmium complex 18d

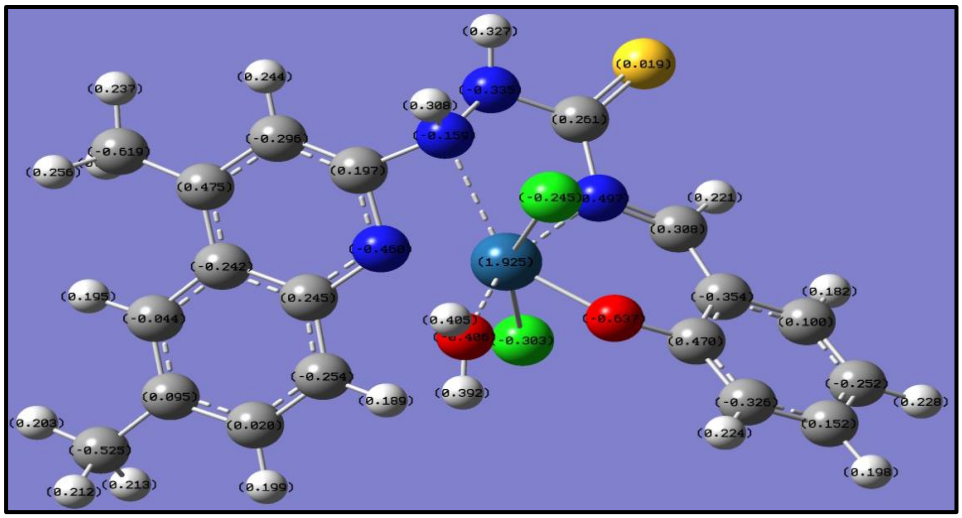

Fig 156 - Optimised geometry of osmium complex 19b

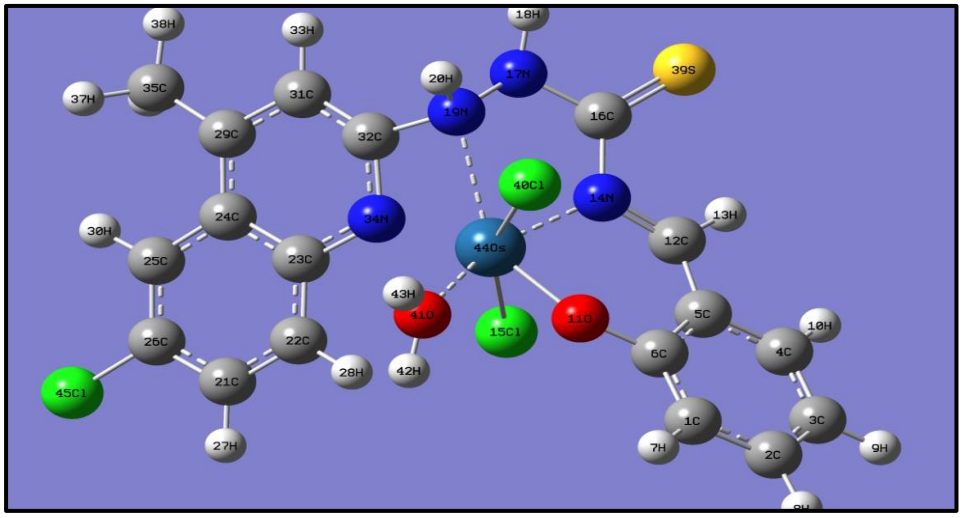

Fig 157 - Optimised geometry of osmium complex 19c

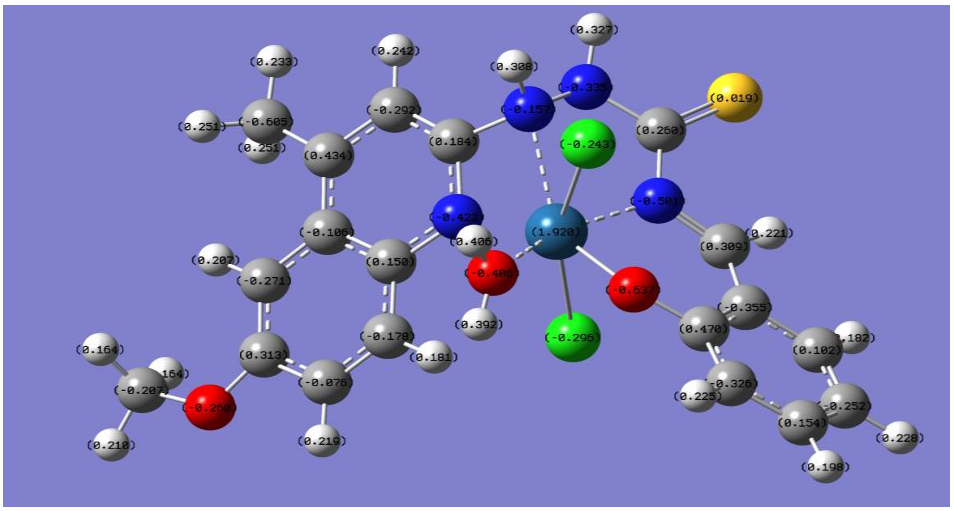

Fig 158- Optimised geometry of osmium complex 19d

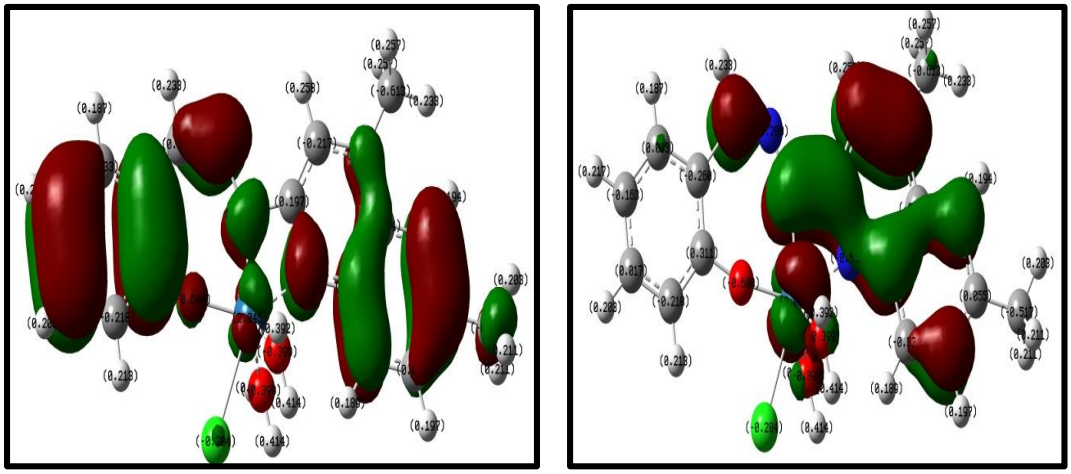

Fig 159 - Frontier molecular orbitals of complex 18b

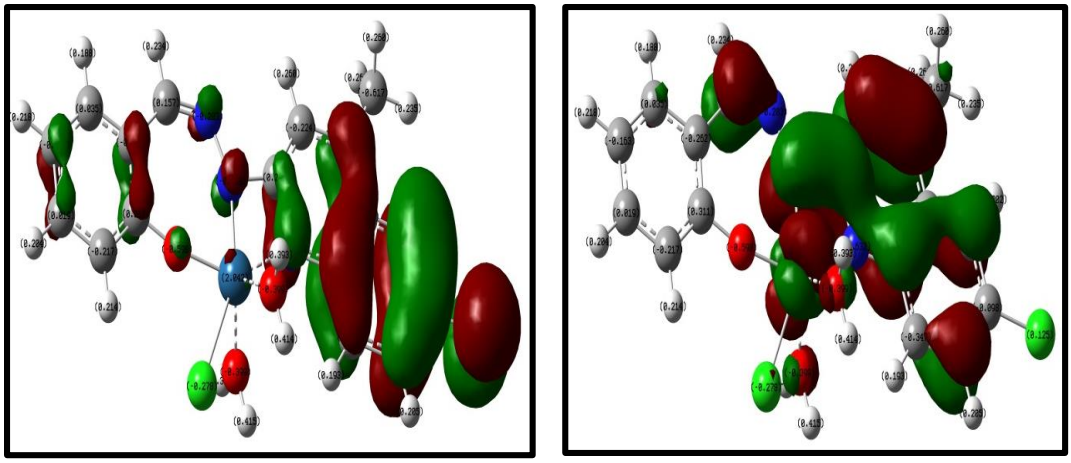

Fig 160 - Frontier molecular orbitals of complex 18c

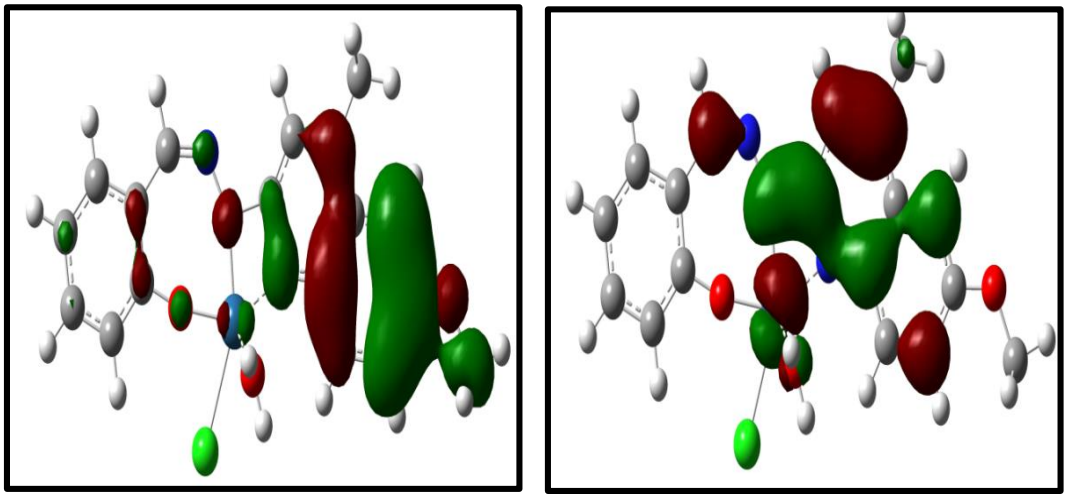

Fig 161 - Frontier molecular orbitals of complex 18d

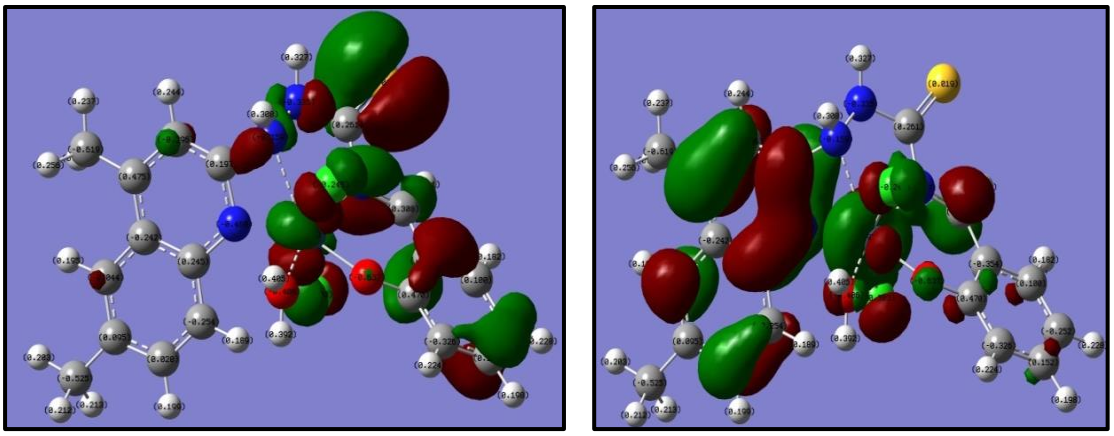

Fig 162 - Frontier molecular orbitals of complex 19b

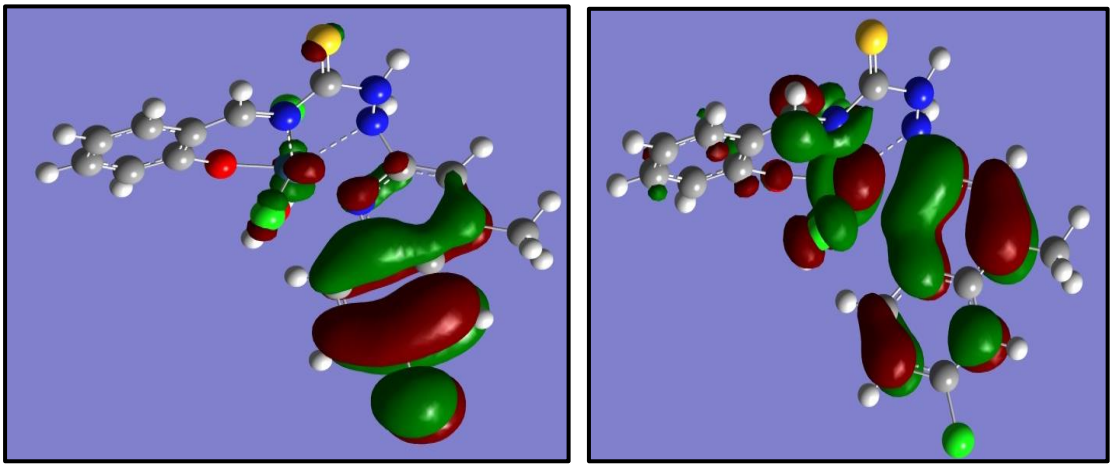

Fig 163 - Frontier molecular orbitals of complex 19c

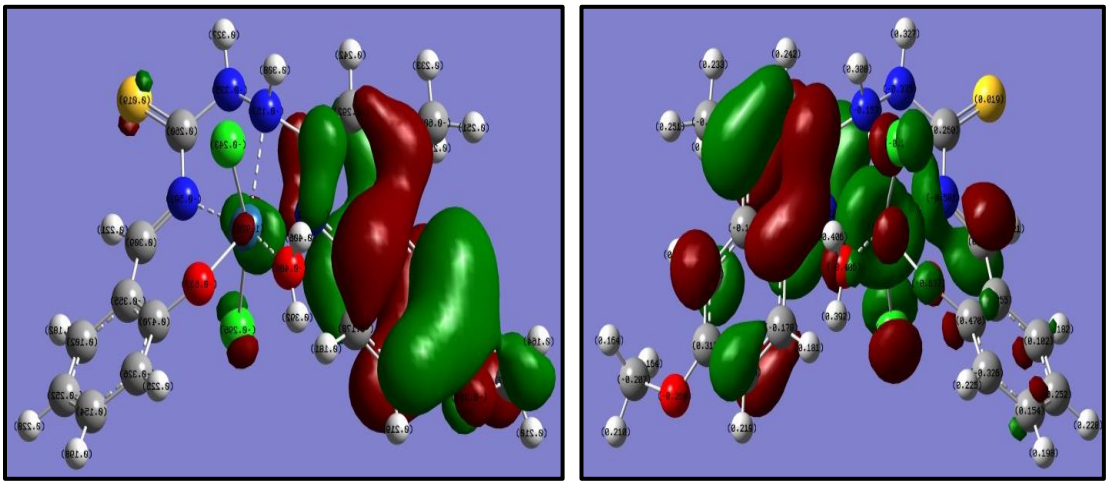

Fig 164 - Frontier molecular orbitals of complex 19d

References

1. R. M. Ramadan, M. S. A. Hamza, A. M. Salem, *Transition Metal. Chem*, **24**, 193 – 197 (1999).
2. T. W. Wong, T.C. Lau, W. T. Wong, *Inorg. Chem*, **38**, 6181 – 6186, (1999).
3. A. Das, F. Basuli, S. M. Peng, S. Bhattacharya, *Polyhedron*, **18**, 2729 – 2736, (1999).
4. P. Majumdar, S. Goswami, S.M. Peng, *Polyhedron*, **18,** 2543 –2548, (1999).
5. B. Panda, A. Chakravorty, *J. of Organomet.Chem*, **690**, 3169 – 3175 (2005).
6. P. Gupta, A. Das, F. Basuli, A. Castineiras, S. Bhattacharya, *Inorg. Chem*, 44(6), 2081-2088 (2005).
7. C. L. Gross, J. L. Brumaghim, G. S. Girolami, *Organometallics*, **26**, 2258-2265 (2007).
8. I. N. Stepanenko, A. A. Krokhin, R. O. John, A. Roller, B. K. Keppler, *Inorg. Chem*, **47**, 7338-7347 (2008).
9. L. K Filak, S. Goschl, S. Hackl, Michael A. Jakupec, V. B. Arion, *Inorganica Chimica Acta***, 393,** 252–260 (2012).
10. L. K. Filak, G. Muhlgassner, *Organometallics*, **30**, 273 – 283 (2011).
11. S. Mandal, D. Seth, P. Gupta, *Polyhedron*, **31,** 167-175 (2011).
12. G. E. Buchel, A. Gavriluta, M. Novak, S. M. Meier, *Inorg. Chem*, **52**, 6273−6285 (2013).
13. L. Chang, K. S. Cho, J. England, C.Y. Wong, *Inorg.chem*, **52 (17),** 9885–9896 (2013).
14. Pariamalpaul, Proc. *Indian Acad. Sci*, **114(4),** 269–276 (2014).
15. M. P. Patel, S. A. Varnum, *Anal. Methods*, **6,** 5818-5828 (2014).
16. P. Pattanayak, D. Patra, A. Burrows, M. F Mahon, S. Chattopadhyay, *J. Chem. Sci.* **125**(1), 51–62 (2013).
17. S. Mandal, S. Mandal, D. K., B. Mukhopadhyay, P. Gupta, *Inorganica Chimica Acta*, **398**, 83-88 (2013).

18. R. G. Alabau, B. Eguillor, J. Esler, M. A. Esteruelas, M. Olivan, C. Xia, *Organometallics*, **33**, 5582-5596 (2014).

19. L. Casarrubios, M. A. Esteruelas, C. Larramona, J. G. Muntaner, E. Onate, M. A. Sierra, *Inorg. Chem*, **54**, 10998−11006 (2015).

20. M. L. Buil, J. J. F. Cardo, M. A. Esteruelas, E. Onate, *J. Am. Chem. Soc*, **138(30)**, 9720−9728 (2016).

21. G. Agonigi, T. Riedel, M. P. Gay, L. Biancalana, E. Onate, F. Marchetti, *Organometallics*, 35, 1046-1056 (2016).

22. M. S Novak, G. E. Buchel, B. K. Keppler, M. A. Jakupec. *J. of Biol. Inorg Chem*. **21**, 347–356 (2016).

23. L. Favereau, A. Makhal, D. Provost, *Phys. Chem. Chem. Phys*, **19(6),** 4778-4786 (2017).

24. G. E Buchel, S. Kossatz, A. Sadique, P. Rapta, M. Zalibera, *Dalton Trans*, **46,** 11925-11941 (2017).

25. H. Sugimoto, K. Kiriyama, S. Itoh, *European. J. of Inorg. Chem*, **2**, 178-185, 2018.

26. P. Zhang, H.Huang, ***Dalton Trans,* 47**, 14841-14854 (2018).

27. A. M. El-Hendawy, H. A. Al-Madfa, A. El-Bindary, A. G. Shoair, M. Diab, *Qatar Univ. Sci. J*, **14 (C)** ,80-87 (1994).